AFCRL-69-0181

OPTICAL PROPERTIES OF 4H, 6H, 15R, 21R, CUBIC SiC

Wolfgang J. Choyke and Lyle Patrick

Westinghouse Research Laboratories
Pittsburgh, Pennsylvania 15235

Contract F 19628-68-C-0272

Project No. 5620
Task No. 562008
Work Unit No. 56200801

FINAL REPORT

Period Covered: 1 April 1968 - 31 March 1969

30 April 1969

Contract Monitor: Herbert C. Lipson
Solid State Sciences Laboratory

Prepared for

AIR FORCE CAMBRIDGE RESEARCH LABORATORIES
OFFICE OF AEROSPACE RESEARCH
UNITED STATES AIR FORCE
BEDFORD, MASSACHUSETTS 01730

ABSTRACT

Optical absorption and reflectivity studies were carried out on a variety of cubic SiC samples. Two additional indirect transitions at 3.55 eV and 4.2 eV have been found. In N-type cubic SiC the inter-conduction band transition X_{1c} to X_{3c} has been accurately located. Results have been compared with recent band calculations of Herman, Van Dyke and Kortum.

Two additional papers were prepared dealing with a general discussion of the dependence of the physical properties on polytype structure and the optical properties of polytypes of SiC.

TABLE OF CONTENTS

I. INTRODUCTION

The objective of this contract was to perform optical experiments which would lead to a further understanding of the band structure of some of the simpler polytypes of SiC.

In general, it would be most satisfying if it were possible to compare the experimental results with a calculation of the band structure derived from first principles. Unfortunately, the present state of the theoretical art does not permit this. In fact, experimenters furnish the theorists with certain key parameters and then a semi-empirical band structure calculation is undertaken. In the case of SiC, the zincblende modification is the one most amenable to a calculation because of its relative simplicity. Fortunately, at the start of this support period, Dr. Frank Herman and his collaborators were interested in performing a calculation on cubic SiC and it was felt that it would be most useful if one could furnish them with new and better experimental results. Indeed, it is for this reason that our effort has been concentrated on cubic SiC and at all stages of the work we have been in close contact with Dr. Herman.

The result of the experimental work on cubic SiC has been the discovery of two additional indirect transitions and a direct inter-conduction band transition for N-type samples. Previously reported structure in the reflectivity at 4.6 eV by Wheeler can now be attributed

to an unknown artifact and is not the onset of the direct transition at the center of the Brillouin zone. The most recent band calculation of Herman, Van Dyke and Kortum, which uses our previously reported value, for the first indirect gap, Γ_{15} to X_{1c} shows no direct transition below 6 eV and bears out the fact that we have seen no structure in the reflectivity until approximately 6 eV. In addition, we are in good agreement with the second indirect transition, L_{3v} to X_{1c} at 3.55 eV, but find a third indirect transition at 4.2 eV which is as yet unidentified. The direct transition threshold seen in N-type samples at 3.05 eV is to be compared with the calculated separation X_{1c} to X_{3c} of 2.7 eV. Such agreement is considered quite satisfactory. A very good start has been made at fulfilling the rather ambitious program of elucidating the band structures of 4H, 6H, 15R, 21R, and cubic SiC, but clearly it will take much more work before even the simplest of the hexagonal and rhombohedral band structures are understood.

II. INSTRUMENTATION

(a) Optical Absorption

The reflectivity of a large band gap semiconductor prior to the onset of the direct transitions is primarily governed by the real part of the complex index of refraction. Furthermore, we can relate the refractive index n, in this region, to $\frac{d\alpha(h\nu')}{d\ h\nu'}$ where α is the ordinary absorption coefficient. For an allowed band-to-band indirect transition, α is proportional to $(h\nu - E_g)^2$ whereas for an allowed direct transition, α is proportional to $(h\nu - E_g)^{1/2}$. From this it can be seen that structure

in the reflectivity might be expected at the onset of a direct transition but not for an indirect transition.

Under these circumstances it is desirable to supplement reflectivity studies with absorption measurements. One would like to extend the ordinary transmission measurements right up to the threshold of the first strong direct transitions. This means making measurements of α of about 50,000 cm^{-1}. To make good measurements in such a regime requires the preparation of single crystals with a thickness of the order of a micron and optical equipment with extremely small light scattering.

Crystals were prepared in the following manner:

(a) Ideally, select a flat sample about 50 to 100μ in thickness which is a single polytype, as deduced from Laue X-ray studies and optical examination.

(b) Make up a small amount of solution of type 650 Owens-Illinois glass resin using 25% by weight of the 650-O-I solid and 75% by weight electronic grade acetone. The resin stock should be kept in a refrigerator at all times and even then it has a limited lifetime. If the solution does not appear absolutely clear, it should be carefully filtered.

(c) Thoroughly clean a 1/2 inch diameter, 1 mm thick, Suprasil II disc having a good optical polish.

(d) Put one drop of resin solution on the Suprasil disc and allow to dry for one hour while covering with a glass jar.

(e) Place flat side of crystal against resin and push on top of crystal with a small teflon-tipped plunger. Put disc and plunger combination on a hot plate which has been pre-heated to about 150°C and allow to cure for one hour. This makes a fairly permanent bond between the sample and the quartz disc.

(f) Attach disc to stainless steel grinding fixture with an appropriate cement. Grind crystal with 600 and 1000 mesh boron carbide on flat plate glass. Frequently, check thickness under the microscope.

(g) Below a thickness of 15μ the boron carbide is discontinued. One now uses 6μ diamond paste on a solder lap. Below a thickness of 5μ, only 1/2μ diamond paste is used. For each stage of polishing, separate solder laps should be used. Below 10μ thickness, microscopic examination becomes most difficult and it is best to rely on actual transmission measurements of the crystal. It should be noted that the crystal is never removed from the disc and measurements are made through the ultra-pure silica disc and resin film. Since neither the ultra-pure silica nor the resin film have any appreciable absorption down to 2000 Å, this was perfectly adequate for our measurements.

Figure 1 is a block diagram of the system used for making the transmission measurements. For reasons already mentioned, one is primarily concerned with the reduction of scattered light and not with high spectral resolution. Normally, three light sources are used, a tungsten ribbon, a xenon high pressure arc, and a deuterium arc. All light source supplies are regulated to 0.1%. The light is chopped at 33 cycles and

pre-filtered by a variety of Corning glass filters. After passing thro[illegible] the double monochromator, the light is further filtered by appropriate liquid cells. An example of such a liquid filter would be a 2 cm diameter and 12 cm long cylinder filled with a $NiSO_4$ solution. The cylinder has two ultra-pure silica end windows which are attached with wax. The light is then re-focussed onto the crystal which is mounted on a machined slide. The slide has two positions, one for the crystal and the other for an open hole. The signal is measured with an RCA 7200 photomultiplier, amplified, phase-detected, and finally read-out on a counter.

(b) Reflectivity

For the experiments conducted during this contract period, it was necessary to perform careful reflectivity measurements from 3000 Å to 1500 Å. A rebuilt Seya-Namioka 1/2-meter grating instrument was used and a block diagram of the system is shown in Fig. 2. For the 3000 Å to 1500 Å region, a Nester-type lamp filled with deuterium is used. A small fraction of the light is fed back to a photomultiplier through a light pipe whose front surface is covered with sodium salicylate. The photomultiplier signal is fed to a feedback network which in turn controls the current to the lamp. In this way the light output is kept constant to about 0.1% for small periods of time. It has been observed that the light output steadily declines with the number of hours the lamp is in operation. This has been traced to a deposit which forms on the outside surface of the MgF_2 lamp-window which is exposed to the intense ultraviolet light. This deposit is easily removed with electronic grade acetone. Recently, a liquid nitrogen cold fringer has been installed

near the lamp window and it has reduced the rate at which the deposit forms on the window. After the light has passed through the entrance slit, it is chopped at 200 cycles by a tuning fork chopper and then dispersed by the 1180 line per mm concave grating. Down to 1100 Å, the grating is an aluminum replica covered with 250 Å of MgF_2. For experiments below 1100 Å, the grating is covered with platinum. Similar considerations hold for all the mirrors in our system.

The light is refocussed onto the sample by the spherical mirror M_2. It would be desirable to use a toroidal mirror at this point to correct for some of the astigmatism. This is particularly pressing when very small samples are used and a good bit of light is lost because of the elongated image. Mirror M_2 can be adjusted for up and down and sideways displacement of the image even while the reflectometer chamber is under vacuum.

When small samples are used, as was the case of cubic SiC, it is desirable not to move the sample during the period of measurement. For this reason we built a reflectometer with a light pipe which rotates in front of the sample as shown in Fig. 2. In the usual system the light pipe rotates concentric with the sample. Despite the fact that the former system is somewhat asymmetric, we have found little difference for the relative values of the reflectivity obtained by either scheme.

The light pipe window is covered with a thin layer of sodium salicylate deposited by means of a fine, oscillating, spray of sodium salicylate diluted in methyl alcohol. The part of the light pipe near the entrance window is aluminized in order not to lose those light rays which are not subject to total internal reflection.

An RCA 8575 photomultiplier was chosen because of its excellent dark-current characteristics and because its peak response is close to that of the sodium salycilate luminescence. To further discriminate against stray light, the RCA 8575 entrance is covered with a Corning 5562 filter which closely matches the peak luminescence of our phosphor and rejects all other visible light.

The maximum output current is held to 10^{-7} amperes so as to assure a very high degree of linearity in our measurements. The signal is amplified, phase-detected, and converted to a digital signal which is read-out on a 50-megacycle counter. At various stages of the electronics, meters are used to insure that no component is being driven into a non-linear region. When all components are working properly, we are able to reproduce our results to better than 0.5%.

Under some circumstances, structure can be enhanced at low temperature. A stainless steel dewar with MgF_2 windows and a separate vacuum system has been constructed and fits either the concentric or the off-axis reflectometer. The dewar is connected to a separate vacuum system which maintains a pressure at the sample of about 5×10^{-7} Torr. Great care is taken to trap out all oil vapors and the sample is further cryopumped by a cold cavity which almost totally surrounds it. The sample can be raised in and out of the beam by means of a vacuum bellows connected to a gear. We judge the dewar to work adequately by the observation that even after several hours of cooling the sample reflectivity in the extreme ultraviolet has not changed much. Finally, it should be noted that the dewar can be used for absorption as well as reflectivity experiments.

III. RESULTS AND PUBLICATIONS

During the sponsorship of this program a number of experiments were brought to a successful conclusion, the results of which have been written up in two scientific papers whose abstracts are repeated here and whose complete texts are given in Appendices A and B.

(A) Optical Absorption in N-Type Cubic SiC

Abstract

Nitrogen doping of cubic SiC increases the optical absorption in two regions. The free-carrier intraband absorption has a wavelength dependence of $\lambda^{2.8}$. An additional narrow band near 3.1 eV is shown to be the direct interband transition from the X_{1c} conduction band to the higher X_{3c} band. The relationship to Biedermann's work on other SiC polytypes is indicated.

(B) Higher Absorption Edges in Cubic SiC

Abstract

In addition to the known indirect absorption edge of cubic SiC at 2.39 eV, measurements of light absorption in thin samples reveal indirect edges at 3.55 and 4.2 eV. Comparisons are made with calculated band separations. The absorption coefficient at 5 eV is 2.4×10^4 cm^{-1}. There is no absorption edge near 4.6 eV as suggested by some reflectivity measurements. The first direct transition appears to be near 6 eV.

In addition, two technical papers of a more general nature were prepared and are given in full in Appendices C and D.

(C) Dependence of Physical Properties on Polytype Structure

Abstract

The physical properties of SiC are classified according to the degree of their dependence on polytype. The relationship of polytype dependence to wave-vector dependence is explained, and is illustrated by a number of examples. The correlation of polytype properties with hexagonality is also considered.

(D) Optical Properties of Polytypes of SiC: Interband Absorption, and Luminescence of Nitrogen-Exciton Complexes

Abstract

A summary is given of the optical absorption in seven polytypes of SiC. Nitrogen-exciton four-particle and three-particle spectra for a number of polytypes are discussed. Combining energies from four-particle and three-particle no-phonon data to yield values for donor ionization energies are reviewed.

IV. RECOMMENDATIONS FOR FUTURE WORK

(a) Study the higher absorption edges in 15R, 21R, and 4H SiC by means of transmission measurements on thin single crystals.

(b) Extend transmission technique to crystalline films grown on Si substrates.

(c) Study the signatures of different surface preparations on optical reflectivity in the U.V.

(d) Make a detailed study of the reflectivity of 6H, 4H, 15R, 21R, and cubic SiC from 4 eV to 20 eV.

(e) Study details in the reflectivity by means of differential techniques.

Dwg. 859A965

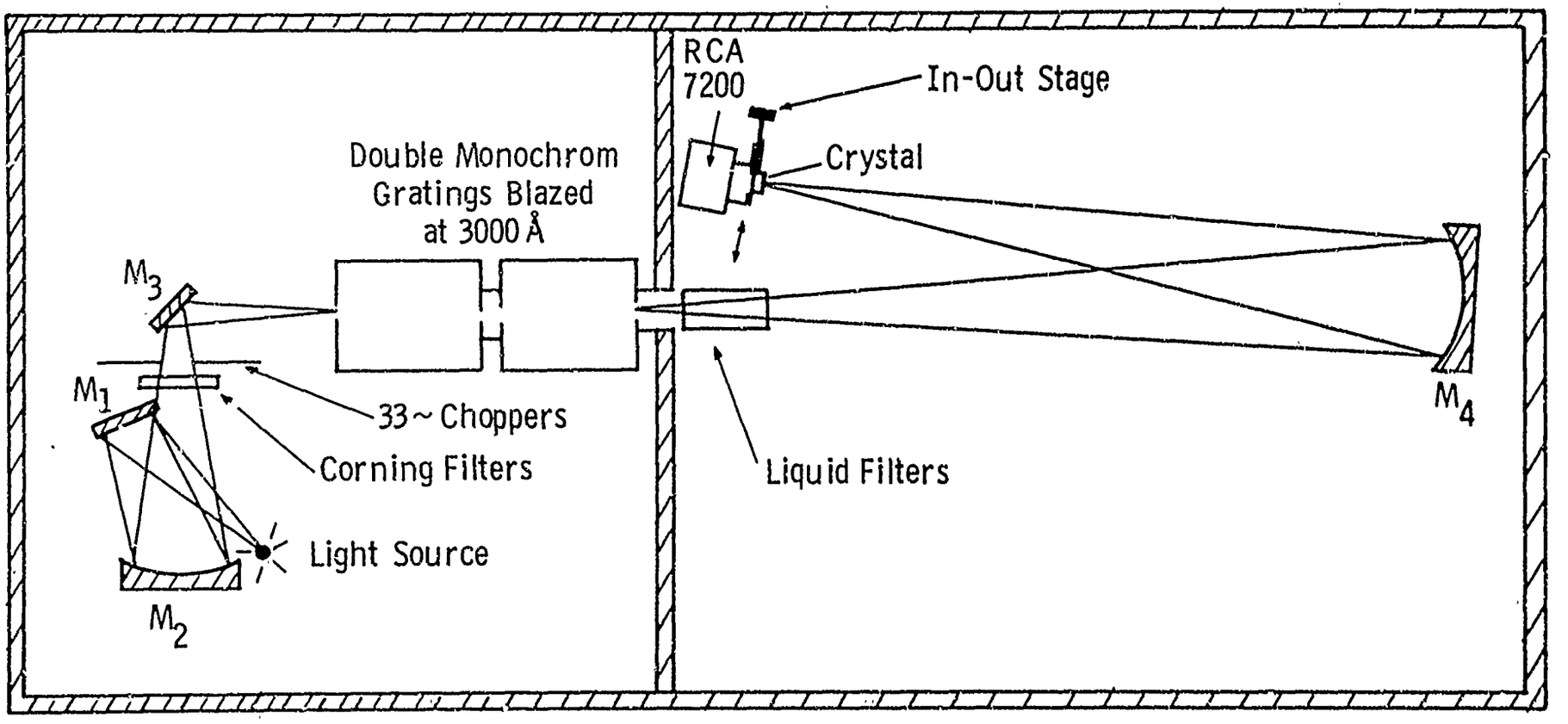

Fig. 1

Dwg. 8594967

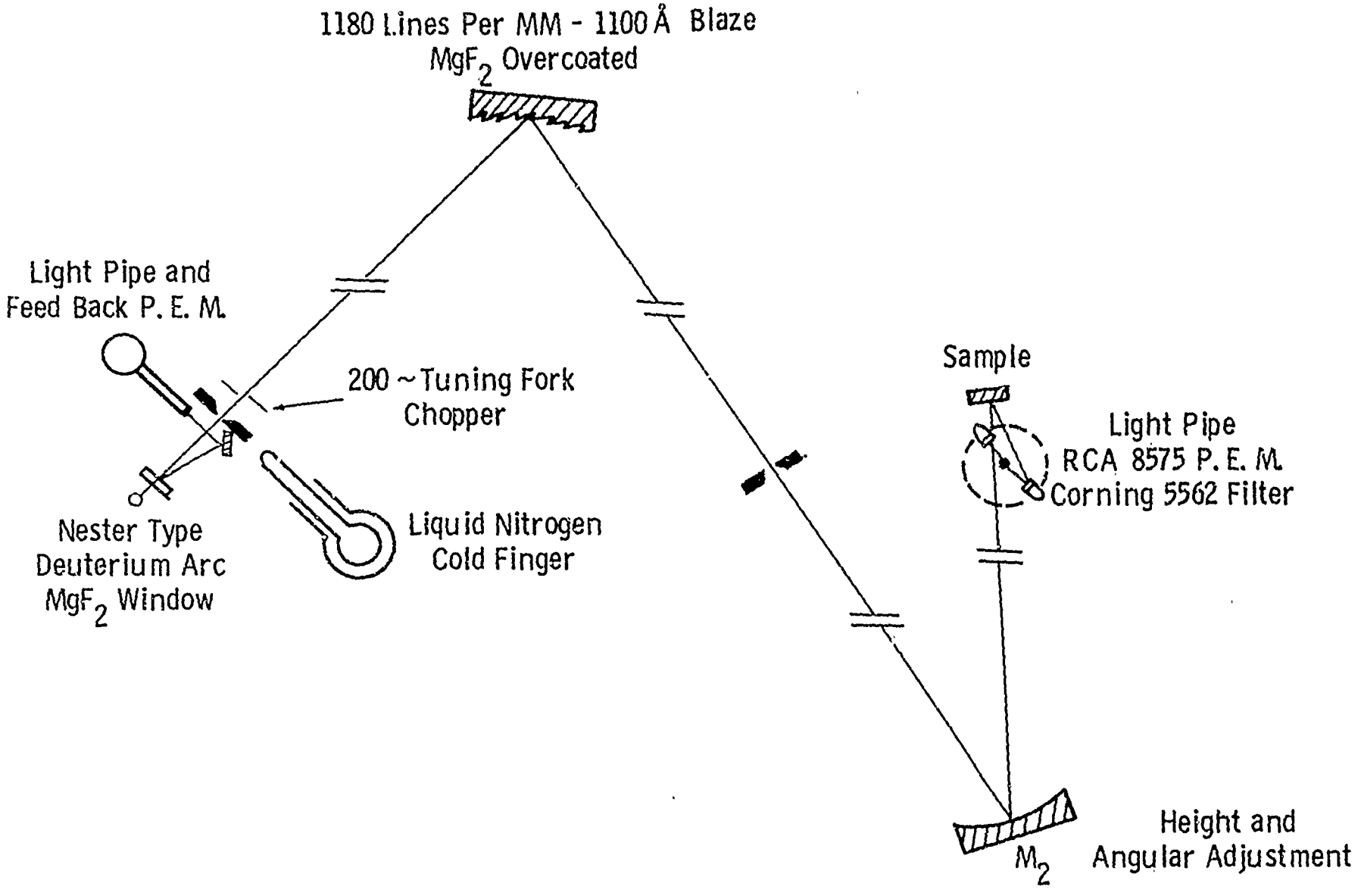

Fig. 2

APPENDIX A -- Optical Absorption in N-Type Cubic SiC

March 7, 1969

OPTICAL ABSORPTION IN N-TYPE CUBIC SiC*

Lyle Patrick and W. J. Choyke

Westinghouse Research Laboratories
Pittsburgh, Pennsylvania 15235

Abstract

Nitrogen doping of cubic SiC increases the optical absorption in two regions. The free-carrier intraband absorption has a wavelength dependence of $\lambda^{2.8}$. An additional narrow band near 3.1 eV is shown to be the direct interband transition from the X_{1c} conduction band to the higher X_{3c} band. The relationship to Biedermann's work on other SiC polytypes is indicated.

---

*The research reported in this paper was sponsored in part by the Air Force Cambridge Research Laboratories, Office of Aerospace Research, under Contract AF 19(628)-68-C-0272, but the report does not necessarily reflect endorsement by the sponsor.

I. INTRODUCTION

We have compared the optical absorption of n-type samples of cubic SiC with that of relatively pure specimens. The n-type samples have additional absorption of two kinds, one of which is the usual free-carrier intraband absorption.[1] The other n-type absorption is a rather narrow band with a maximum at 3.1 eV, and can be attributed to the transition of electrons in the X_{1c} conduction band to the higher X_{3c} band. This is an allowed direct transition.

Such interband transitions in n-type crystals were observed by Biedermann in several SiC polytypes.[2] They are responsible for the well-known colors of nitrogen-doped samples, e.g. green 6H and yellow 15R. The cubic n-type interband absorption differs from those reported for the other polytypes in three respects. (1) No part of the absorption band lies in the visible range, hence it does not contribute to crystal color. (2) The direct n-type absorption falls within the energy range of the intrinsic indirect interband absorption. (3) Only a single isotropic absorption band is found, because of the high symmetry of the cubic SiC band structure.

The lower limit of the interband transitions, about 3.05 eV, yields a value of the $X_{1c} - X_{3c}$ band separation which is in good agreement with some of the calculated values.[3,4] We discuss the possibility of distinguishing between absorption by electrons in the conduction band and by those bound to donor atoms. The wavelength

dependence of the free-carrier intraband absorption yields information on the electron-scattering mechanisms. Either polar or impurity scattering (or both) appear to be consistent with the experimental results.

II. EXPERIMENTAL

A. Crystal Preparation

All measurements were made on vapor-grown crystals that originated as cubic overgrowths on hexagonal crystals,[5] the overgrowths being deposited during the cooling period of the crystal growing furnace.[6] The hexagonal parts were ground off, leaving small but good quality single crystals of cubic SiC, as shown by Laue transmission X-ray pictures. Various pressures of nitrogen were used in the furnace during crystal growth. No electrical measurements were made on the small cubic crystals, but measurements on hexagonal crystals grown in the same furnace show donor densities ranging from $10^{17}/cm^3$ at the lowest nitrogen pressures to $10^{19}/cm^3$ or more at the highest.

B. Experimental Results

The absorption of an n-type crystal is compared with that of a pure crystal in Fig. 1. The relatively pure A crystal probably has a donor density of order $10^{17}/cm^3$, but no evidence of the donors is found in the optical measurements. It has an indirect absorption edge at 2.39 eV.[7] The n-type B crystal is thought to have a donor density of order $10^{19}/cm^3$. Other crystals were found to have different intensities of the 3.1 eV absorption band, and the intensity correlated qualitatively

with the nitrogen pressure in the crystal-growing furnace, and with a color change to be described later.

The additional n-type absorption near 3.1 eV, $\Delta\alpha = \alpha_B - \alpha_A$, is plotted in Fig. 2. It is an asymmetric band, but the shape cannot be determined accurately because of the uncertainty in $\Delta\alpha$ in the wings. Because of the difficulty of measuring absolute absorption coefficients on small crystals, the difference between the two crystals, $\Delta\alpha$, is not reliable when it is much smaller than α_A. At 4.2°K the 3.1 eV band narrows considerably and moves to a slightly higher energy. At 77°K the width of the band is close to that at 4.2°K.

III. DISCUSSION

A. Interband Absorption

Cubic SiC has the zincblende structure. Both theory and experiment suggest that the extra interband absorption in n-type samples should be attributed to direct transitions from the X_{1c} conduction band to the higher X_{3c} band.[8] Recent band calculations by Herman, Van Dyke, and Kortum show an $X_{1c} - X_{3c}$ separation of about 2.7 eV, compared with about 3.05 eV for the observed absorption edge (Fig. 2). Experimentally, the energies of the phonons emitted in the indirect exciton recombination transitions were measured.[7] These phonons conserve crystal momentum, and therefore have the same $\underset{\sim}{k}$ values as the conduction band minima. The degeneracy of the transverse phonon modes in the exciton spectrum shows that the conduction band minima lie in directions of high symmetry. The L positions are then excluded by noting that the

phonon energies are different from those found for L in Raman scattering experiments.[9] Thus, we conclude that the conduction band minima are very likely at X.

A similar transition, also at X, is observed in n-type GaP at 0.4 eV.[10] Bassani remarks that the $X_{1c} - X_{3c}$ splitting, which is due to the antisymmetric portion of the crystal potential, is large for small atoms.[11] Biedermann made absorption measurements on n-type samples of several other SiC polytypes, and attributed the absorption to direct transitions from the conduction band to higher bands.[2] However, the bands between which the transitions take place have not been identified for these polytypes, because the exact positions of the conduction band minima are not yet known.

In recent measurements[12] on the donor-induced transitions in 6H SiC, an attempt was made to distinguish between absorption by electrons bound to donors and by conduction band electrons. In cubic SiC we find only a single absorption band, which narrows and shifts to higher energy at $4.2^{\circ}K$. The shift of about 15 meV is possibly due to a change in interband separation. The band shape and the band narrowing at low temperature are not unlike those observed for the inter-valence-band transitions between bands 1 and 3 in p-type Ge. A comparison of experimental and calculated absorption was possible for Ge,[13,14] but it requires band parameters which are not known for cubic SiC. In any case, the absorption band shape is not well known experimentally, as noted above, and it is not expected to be very different for electrons bound to donors or in the conduction band.[13] Thus, we think that the

experimental results do not answer the question of the initial location of the electrons.

If we examine the data for the 6H absorption band in Ref. 12 we find that a thermal shift in the interband spacing and thermal broadening can qualitatively explain the observed temperature dependence. Hence, we feel that the presence of two distinct absorption mechanisms has not yet been shown. In both the cubic and the 6H SiC data, impurity banding may blur the distinction between bound and free electrons, for the donor densities were of order $10^{19}/cm^3$.

B. Intraband Absorption

The free-carrier intraband absorption (0.6 to 2.0 eV) is similar to that found for other polytypes by Biedermann[2] and others.[15] It is customary to plot this portion of the absorption on log-log paper to find the index s that best describes the wave-length dependence in the formula $\alpha = \text{const.}\ \lambda^s$. The classical value, $s = 2$, is not found for the photon energies employed here, which are large compared with either the thermal energy kT or the SiC phonon energies. Instead, s is expected to depend on the electron-scattering mechanism that transfers the absorbed energy to the lattice. Visvanathan finds $s = 2.5$ for polar mode scattering, and $s = 3$ for impurity scattering.[16] For the data in Fig. 1 we find $s = 2.8$, in fair agreement, considering theoretical and experimental uncertainties, with either or both of these mechanisms.

For the room-temperature electron mobility in cubic SiC, polar mode scattering is unimportant because of the high LO phonon energy of

0.12 eV.[9] However, in optical absorption, the intermediate state electron is effectively a "hot" electron, having an energy > 0.6 eV, thus making emission of LO phonons an important mechanism of energy loss.

C. Crystal Color

The coloring of SiC crystals by nitrogen has often been noted. The common 6H and 15R polytypes are transparent when pure, but green and yellow respectively when enough of the donor nitrogen is present. Presumably, any other donor would be equally effective. Crystals of these polytypes are uniaxial, and Biedermann's measurements show a strong dichroism. However, the typical SiC crystal platelet has its large dimension perpendicular to the c axis, so that only the ordinary ray color is observed unless windows are polished on the narrow crystal edges. The complexity of these absorption bands is a reflection of the complex band structure of such polytypes as 6H and 15R, which, in turn, has made it difficult to locate the positions of their conduction band minima precisely. In contrast, cubic SiC has the relatively simple zincblende structure, and, consequently, a simple isotropic absorption band.

Unlike the other polytypes, cubic SiC is not colored by the n-type interband absorption, for 3 eV is beyond the range of sensitivity of the eye. Nevertheless, strong nitrogen doping is observed to change the crystal color from a pale canary yellow to a greenish yellow, as previously noted.[17] The yellow of pure crystals is due to the intrinsic but weak absorption in the blue. The shift towards the green in nitrogen-doped crystals is due to the free-carrier intraband absorption, which absorbs red preferentially.

ACKNOWLEDGMENT

We wish to thank R. B. Campbell, of Westinghouse Astronuclear Laboratory, for supplying us with the crystals used in this experiment.

REFERENCES

1. F. Stern, in Solid State Physics, edited by F. Seitz and D. Turnbull (Academic Press Inc., New York, 1963), Vol. 15, p. 299. See p. 374.
2. E. Biedermann, Solid State Comm. 3, 343 (1965).
3. F. Herman, J.P. Van Dyke and R.L. Kortum, Materials Research Bulletin, to be published.
4. F. Bassani and M. Yoshimine, Phys. Rev. 130, 20 (1963).
5. Supplied by R.B. Campbell, Westinghouse Astronuclear Laboratory.
6. W.F. Knippenberg, Philips Res. Repts. 18, 161 (1963). See p. 263.
7. W.J. Choyke, D.R. Hamilton and Lyle Patrick, Phys. Rev. 133, A1163 (1964).
8. The optical transition is allowed. The group product of X_1 and X_3 is X_3. Dipole transitions are X_3 or X_5.
9. D.W. Feldman, James H. Parker, Jr., W.J. Choyke and Lyle Patrick, Phys. Rev. 173, 787 (1968).
10. R. Zallen and W. Paul, Phys. Rev. 134, A1628 (1964).
11. F. Bassani, in Semiconductors and Semimetals, edited by R.K. Willardson and A.C. Beer (Academic Press Inc., New York, 1966), Vol. 1, p. 21. See p. 67.
12. G.B. Dubrovsky and E.I. Radovanova, Physics Letters 28A, 283 (1968).
13. A.H. Kahn, Phys. Rev. 97, 1647 (1955).
14. E.O. Kane, J. Phys. Chem. Solids 1, 82 (1956).
15. B. Ellis and T.S. Moss, Proc. Roy. Soc. (London) 299, 393 (1967); R. Groth and E. Kauer, Phys. Stat. Sol. 1, 445 (1961).
16. S. Visvanathan, Phys. Rev. 120, 376, 379 (1960).
17. W.E. Nelson, F.A. Halden and A. Rosengreen, J. Appl. Phys. 37, 333 (1966).

FIGURE CAPTIONS

Fig. 1 Absorption spectra of cubic SiC crystals A (dashed) and B (solid) at 300°K. Crystal A is relatively pure; crystal B is strongly n-type (perhaps $10^{19}/cm^3$ donors).

Fig. 2 Difference of crystal A and B absorption coefficients ($\Delta\alpha$) near 3.1 eV, at 300°K (solid) and at 4.2°K (dashed).

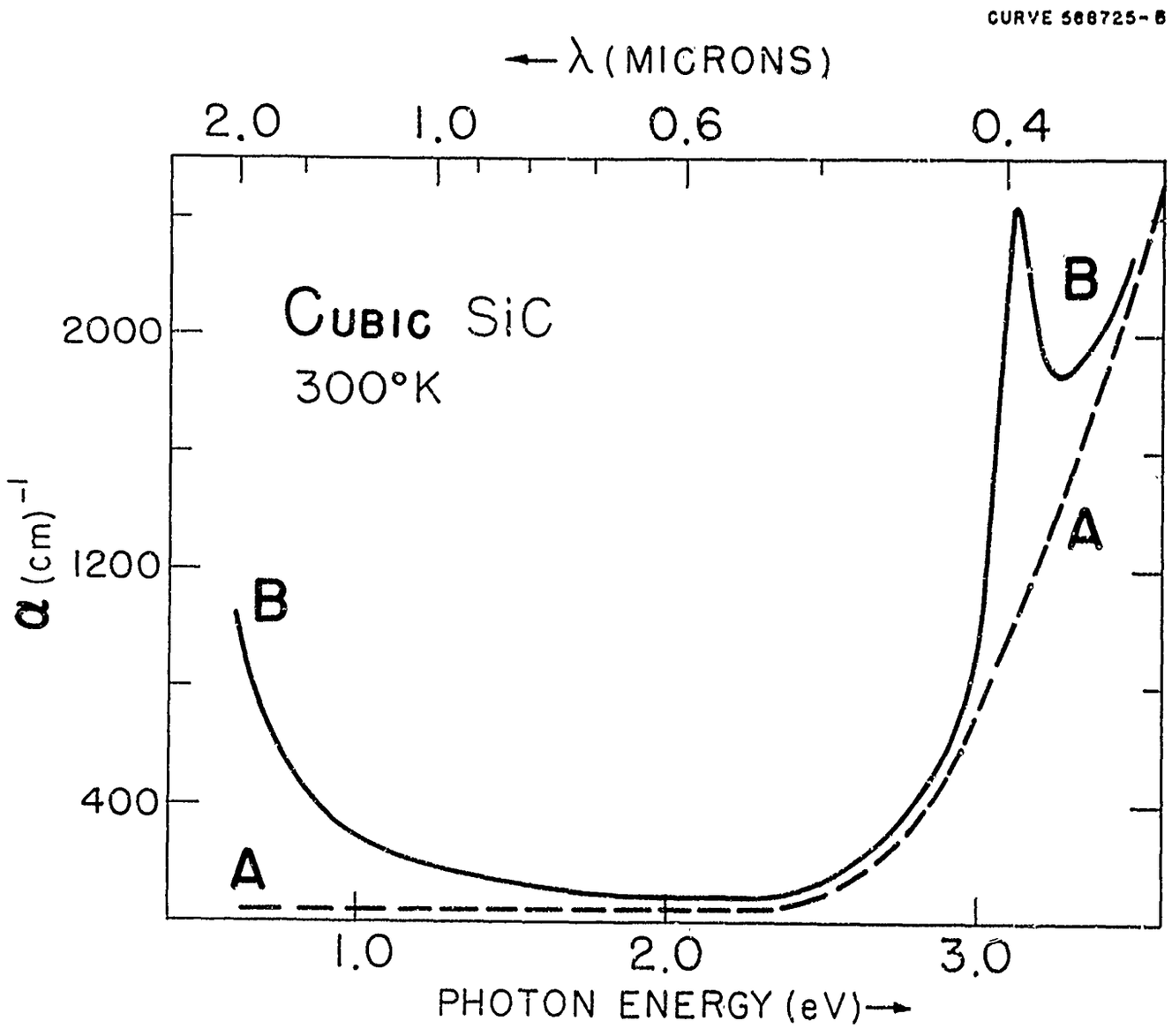
CURVE 568725-B
← λ (MICRONS)
2.0
1.0
0.6
0.4
CUBIC SiC
300°K
B
A
B
A
2000
1200
400
α (cm)⁻¹
1.0
2.0
3.0
PHOTON ENERGY (eV)→

Fig. 1

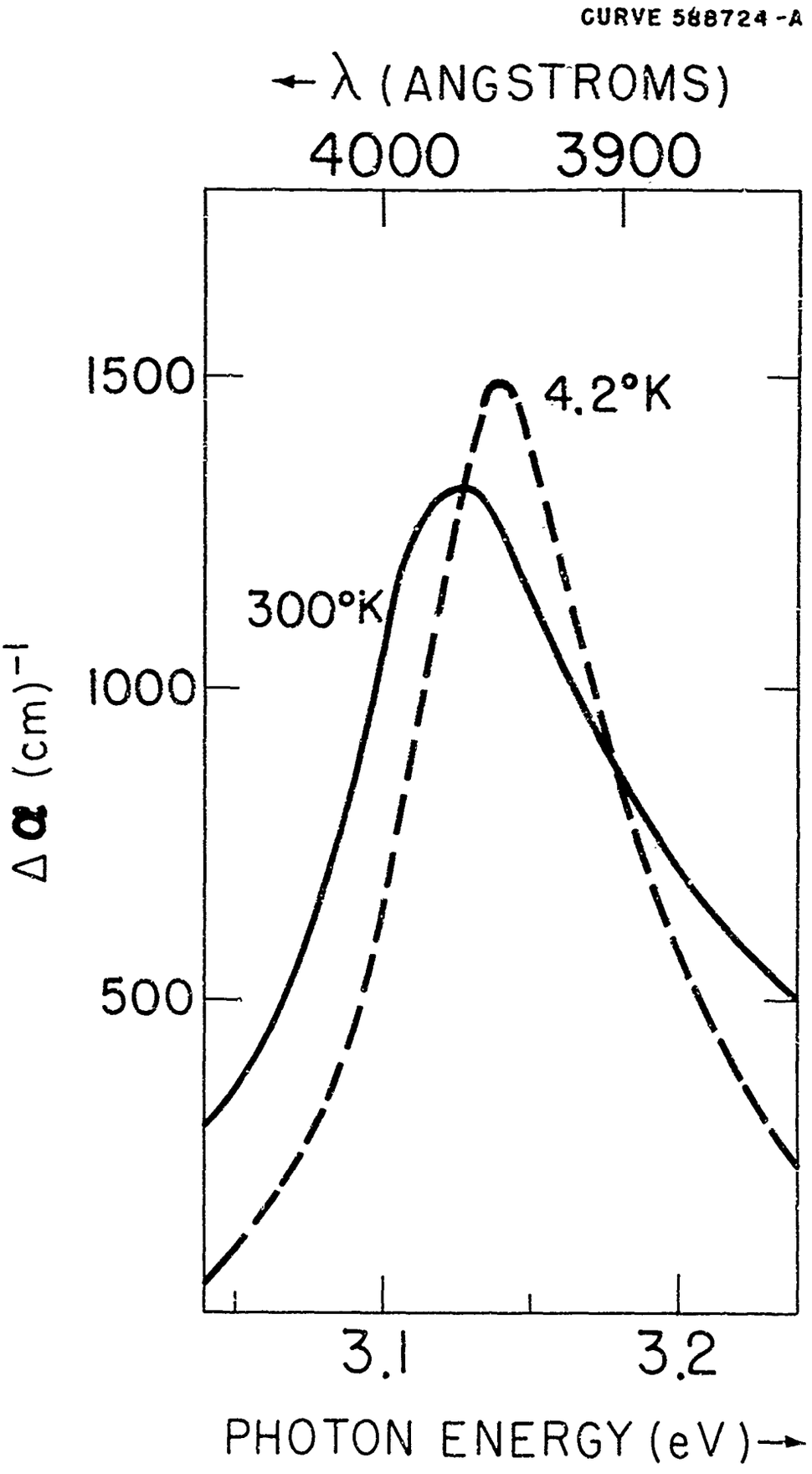
CURVE 588724-A
← λ (ANGSTROMS)
4000
3900
1500
1000
500
4.2°K
300°K
Δα (cm)⁻¹
3.1
3.2
PHOTON ENERGY (eV) →

Fig. 2

BLANK PAGE

APPENDIX B -- Higher Absorption Edges in Cubic SiC

April 15, 1969

HIGHER ABSORPTION EDGES IN CUBIC SiC*

W. J. Choyke and Lyle Patrick

Westinghouse Research Laboratories
Pittsburgh, Pennsylvania 15235

Abstract

In addition to the known indirect absorption edge of cubic SiC at 2.39 eV, measurements of light absorption in thin samples reveal indirect edges at 3.55 and 4.2 eV. Comparisons are made with calculated band separations. The absorption coefficient at 5 eV is 2.4×10^4 cm^{-1}. There is no absorption edge near 4.6 eV as suggested by some reflectivity measurements. The first direct transition appears to be near 6 eV.

---

*The research reported in this paper was sponsored in part by the Air Force Cambridge Research Laboratories, Office of Aerospace Research, under Contract No. F19628-68-C-0272, but the report does not necessarily reflect endorsement by the sponsor.

I. INTRODUCTION

We have measured the absorption of light in cubic SiC from 2.35 to 5.0 eV, a region in which there are three indirect absorption edges and no direct edges. We have also made preliminary measurements of the reflectivity which show that the first direct transitions occur near 6 eV, not at 4.6 eV as previously thought.

Cubic SiC has the zincblende structure, which is considerably simpler than that of the common 6H and 15R polytypes,[1] a fact evident in many experimental results. However, experimental work has been hampered by the difficulty of growing adequate-sized crystals of cubic SiC, a low-temperature polytype. Our measurements were made on both vapor-grown and solution-grown single crystals whose origin and preparation will be discussed.

Because of the simple structure, cubic SiC is the polytype for which most energy-band calculations have been made,[2,3] and it is therefore the logical one for UV reflectivity measurements with which to test and assist the semi-empirical calculations. However, the range in which absorption takes place only through indirect (phonon-assisted) transitions is more than 3 eV, and such transitions do not generate structure in the reflectivity.[4] Hence, an adequate test of band calculations requires one to supplement reflection with absorption measurements to locate the indirect edges. The use of thin samples,

obtained by grinding and polishing, enabled us to find two additional edges beyond the range of photon energies used in earlier measurements of the first absorption edge.[5] Similar additional indirect edges were previously reported for 6H SiC.[6]

Earlier measurements of the low-temperature luminescence,[5] and of the absorption in n-type samples,[7] identified the 2.39 eV indirect transitions as $X_{1c} - \Gamma_{15v}$. We now find a second absorption edge at 3.55 eV, which is close to the value suggested for the transitions $X_{1c} - L_{3v}$ by the recent calculations of Herman, Van Dyke, and Kortum.[2] Possible identification of a third indirect edge at 4.2 eV will be discussed.

For indirect transitions an approximate but simple method of analyzing the absorption data will be outlined before the experimental results are given.

II. INDIRECT TRANSITIONS

The smallest energy gap of cubic SiC is 2.39 eV at 4.2°K,[5] and the absorption edge has the shape expected for indirect transitions in which excitons are created.[8] However, the detailed theory cannot be applied to successive indirect transitions at higher energies because lifetime broadening makes it impossible to observe the exciton and phonon structure. In addition, the usual formula has energy denominators which can be considered constant only over a very limited range of photon energies. We wish to analyze absorption data from 2.39 to 5.0 eV, a range in which the unknown energy denominators may vary by factors of five or ten. We therefore cannot hope to extract a great number of

parameters from our data. However, we are primarily interested in locating the approximate positions of absorption thresholds, and that is an easier task.

In examining the similar problem in 6H SiC it was found that a plot of $\alpha^{1/2}$ versus photon energy showed distinct linear sections, and that the data could be fitted by the simple formula

$$\alpha = \sum \alpha_i = \sum A_i (h\nu - E_{gi})^2$$

where α is the absorption constant in cm^{-1}, the A_i are constants, and the E_{gi} are energy thresholds. This is an approximate formula in which all fine structure is disregarded.(6) The true energy thresholds were estimated to be somewhat higher when allowance was made for exciton and phonon structure. The problem in cubic SiC is the same, and the same procedure will again be used to analyze the data.

III. EXPERIMENTAL PROCEDURES

A. Sample Preparation

Measurements were made on six vapor-grown crystals obtained from R.B. Campbell of Westinghouse Astronuclear Laboratory, and one solution-grown crystal kindly supplied by A. Rosengreen of Stanford Research Institute.

The vapor-grown crystals originated as cubic overgrowths on hexagonal crystals, the overgrowths forming during the cooling period of the crystal-growing furnace.(9) The hexagonal parts were ground off, leaving small but good quality single crystals of cubic SiC, as shown

by Laue transmission X-ray pictures. Strongly n-type crystals were not used, for they have a donor-induced absorption band which overlaps and is sometimes comparable in strength with the intrinsic absorption.[7]

Thin specimens were needed for measurements at high photon energies. These were obtained, down to 3.7μ, by grinding and polishing crystals bonded to Suprasil II[10] with Type 650 O-I Glass Resin.[11] The final thickness of a ground specimen was determined, probably within 10%, by comparing its absorption with that of a sample of measured thickness, in a spectral region in which good absorption measurements could be made on both.

The Stanford Research Institute crystal, grown from Si solution,[12] was approximately 12μ thick, as measured by its transmission interference fringes.[13] However, there are growth terraces on the surfaces, so the thickness may vary from about 11 to 13μ. It had only a very weak donor-induced absorption near 3.1 eV. In comparing absorption spectra, no differences between vapor-grown and solution-grown crystals were detected, nor between polished and unpolished crystals.

B. Measurement of Transmitted Light

The relative transmission of the samples was measured by a standard comparison method. We used a Jarrel-Ash double monochromator with gratings blazed at 3000 Å. The light source was a regulated xenon arc, and scattered light was reduced by the use of Corning filters and, above 3.8 eV, by various combinations of liquid UV filters.[14] At the higher energies it becomes increasingly hard to find good filter combinations.

Samples of the proper thickness were chosen to give a convenient range of optical densities for each spectral region. The samples were at room temperature for all measurements. Cooling the sample does not improve the resolution at the higher absorption edges, for the resolution is limited not by thermal, but by lifetime broadening.

IV. EXPERIMENTAL RESULTS

To cover a wide energy range it was necessary to make measurements on samples of various thicknesses. The results of all measurements were combined to plot Fig. 1, which shows $\alpha^{1/2}$ versus photon energy, the plot commonly used for indirect transitions. The absorption coefficient at 5 eV is about 2.4×10^{4} cm^{-1}. Figure 1 shows three numbered linear segments (solid lines) connected by transition regions (dotted). The linear parts are extrapolated (broken lines) to indicate how one obtains the additional absorption for fitting each linear segment in turn. The procedure is given more fully in Ref. 6.

The data have been fitted by Eq. 1, using the values of A_i and E_{g_i} shown in Table I. Experimental points fall within the width of the solid lines. At high energies, however, the 10% uncertainty in sample thickness results in a 10% uncertainty in absolute absorption coefficient. This does not affect the values of the E_{gi}, in which the uncertainty is due to our inability to resolve exciton and phonon structure. As in Ref. 6, we estimate the true E_{gi} to be somewhat higher than the fitted values. The third column of Table I shows the estimated values that we use for comparison with the calculated band structure.

Notice that the values of the A_i increase with increasing E_{gi}. This is, in part, the way in which our simple formula takes into account the fact that, in the complete formula for the second-order transitions, the energy denominators decrease as the photon energy increases. The same effect was observed in fitting the 6H SiC absorption.[6]

V. DISCUSSION

A. Comparison with Reflectivity Results

An important result is that we observe no additional absorption beginning at 4.6 eV, where Wheeler reported structure in the reflectivity.[15] The structure was tentatively interpreted as a direct transition, but now appears to be an artifact due to surface properties or to the experimental procedure. We also made reflectivity measurements in this region, but we observed no structure below 6.0 eV, where there is a reflectivity peak.[16] At photon energies too low for direct transitions, the reflectivity is determined largely by the real part of the dielectric constant,[4,6] hence the first reflectivity peak at 6.0 eV is thought to correspond closely to the minimum energy of direct transitions.

We may note here that Wheeler also reported structure in the reflectivity of 6H SiC at 4.6 eV.[15] Our absorption measurements for this polytype showed an absorption component beginning near 4.6 eV, with an energy dependence apparently like that of an indirect transition.[6] Since indirect transitions do not generate structure in the reflectivity we concluded that we could not rule out the possibility

that the 4.6 eV edge was direct. It now appears likely that Wheeler's 6H reflectivity structure at 4.6 eV is also an artifact, with a similar origin to the cubic structure, and that the absorption edge we observed is indeed indirect.

B. Comparison with Calculated Band Structure

Herman, Van Dyke, and Kortum have made an OPW calculation of the energy-band structure of cubic SiC, using Kohn-Sham exchange.[2] This calculation shows good agreement with two observed band separations, namely 2.35 eV for $X_{1c} - \Gamma_{15v}$, the indirect band gap, and 3.0 eV for $X_{3c} - X_{1c}$, the donor-induced absorption edge.[7] It also shows an $X_{1c} - L_{3v}$ separation close to our experimental value of 3.55 eV for the second indirect edge. However, the next indirect transition suggested by the calculated band structure is $L_{1c} - \Gamma_{15v}$ at about 5.6 eV, much higher than the observed third edge at 4.2 eV. If the calculated value were reduced to 4.2 eV by adjusting L_{1c}, to force agreement with experiment, it would also reduce the calculated $L_{1c} - L_{3v}$ direct transition to 5.4 eV, and we do not observe a peak in reflectivity at this energy. Thus, the 4.2 eV absorption edge remains unidentified.

ACKNOWLEDGMENT

We wish to thank R.B. Campbell of Westinghouse Astronuclear Laboratory and A. Rosengreen of Stanford Research Institute for supplying the crystals used in this experiment.

TABLE I -- Parameters used in fitting Fig. 1, and estimated values of E_g when some allowance is made for exciton structure.

A (10^3 $cm^{-1}eV^{-2}$)	Fitted E_g (eV)	Estimated E_g (eV)
1.5	2.31	2.35
2.7	3.48	3.55
9.6	4.15	4.20

REFERENCES

1. A.R. Verma and P. Krishna, Polymorphism and Polytypism in Crystals (John Wiley & Sons, Inc., New York, 1966).
2. F. Herman, J.P. Van Dyke and R.L. Kortum, Mat. Res. Bull. 4, S167 (1969).
3. F. Bassani and M. Yoshimine, Phys. Rev. 130, 20 (1963).
4. F. Stern, in Solid State Physics, edited by F. Seitz and D. Turnbull (Academic Press, Inc., New York, 1963), Vol. 15, p. 299. See p. 333.
5. W.J. Choyke, D.R. Hamilton and Lyle Patrick, Phys. Rev. 133, A1163 (1964).
6. W.J. Choyke and Lyle Patrick, Phys. Rev. 172, 769 (1968).
7. Lyle Patrick and W.J. Choyke, to be published.
8. T.P. McLean, in Progress in Semiconductors (Heywood and Co., Ltd., London, 1960), Vol. 5, p. 55.
9. W.F. Knippenberg, Philips Res. Repts. 18, 161 (1963). See p. 263.
10. From Amersil Quartz Division of Englehard Industries, Inc.
11. Obtained from Owens-Illinois Technical Center.
12. W.E. Nelson, F.A. Halden and A. Rosengreen, J. Appl. Phys. 37, 333 (1966).
13. The dielectric constant was assumed to be close to that of 6H SiC as given in W.J. Choyke and Lyle Patrick, J. Opt. Soc. Am. 58, 377 (1968).
14. M. Kasha, J. Opt. Soc. Am. 38, 929 (1948).
15. B.E. Wheeler, Solid State Commun. 4, 173 (1966).
16. We are continuing the reflectivity experiments in order to verify other reported structure and, if possible, to improve on previous work.

FIGURE CAPTION

Fig. 1 Plot of $\alpha^{1/2}$ versus $h\nu$ over the whole range of measurements, showing three linear portions. Measured values fall on straight-line segments (solid), or in transitional regions (dotted). The first two straight-line segments are extrapolated (dashed) to emphasize the beginning of additional absorption.

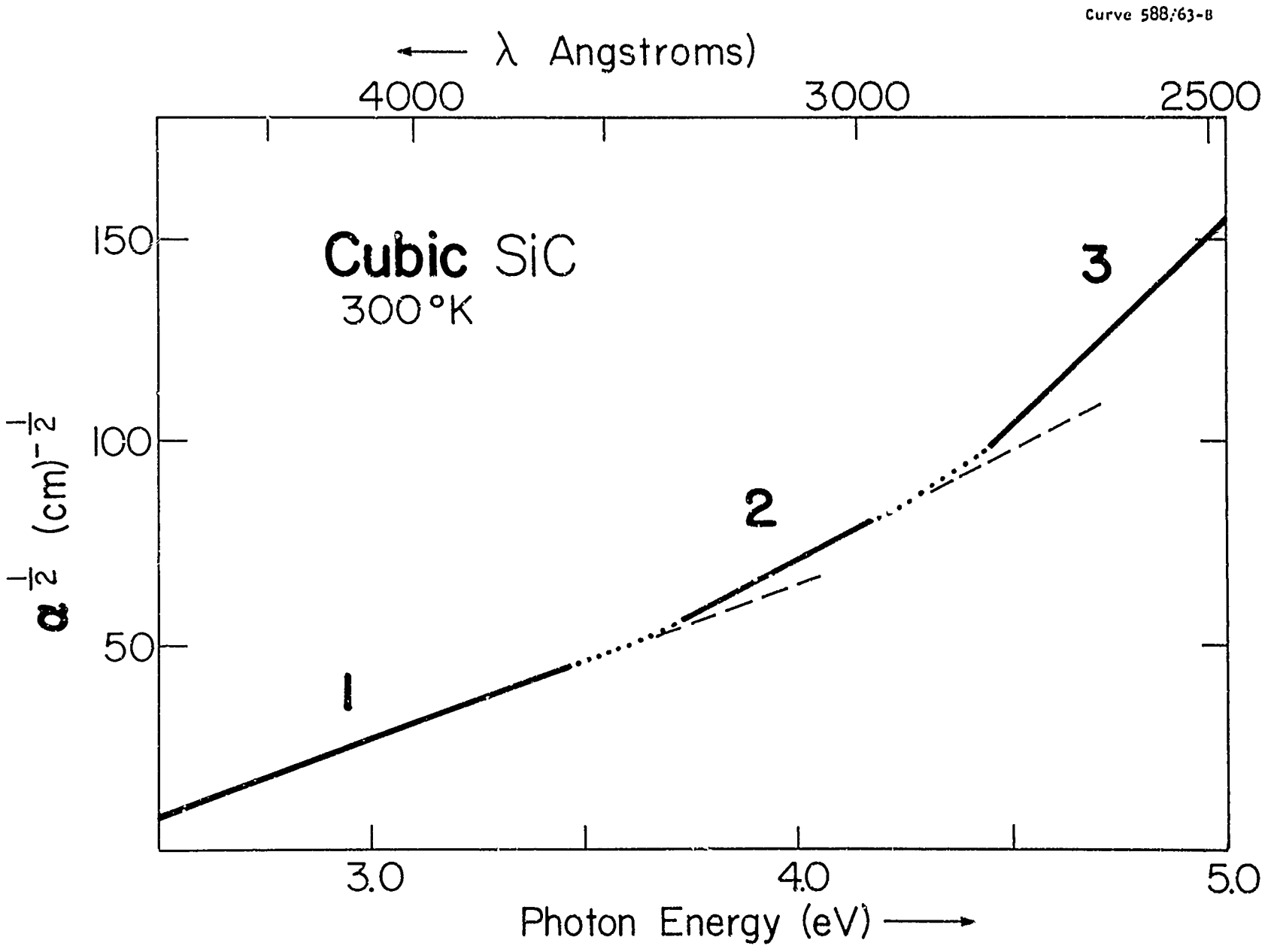
Curve 588/63-B
← λ Angstroms)
4000
3000
2500
Cubic SiC
300°K
150
100
50
1
2
3
$\alpha^{\frac{1}{2}}$ (cm)$^{-\frac{1}{2}}$
3.0
4.0
5.0
Photon Energy (eV) →

Fig. 1

BLANK PAGE

APPENDIX C -- Dependence of Physical Properties on Polytype Structure

August 28, 1968

DEPENDENCE OF PHYSICAL PROPERTIES ON POLYTYPE STRUCTURE*

Lyle Patrick

Westinghouse Research Laboratories
Pittsburgh, Pennsylvania 15235

Abstract

The physical properties of SiC are classified according to the degree of their dependence on polytype. The relationship of polytype dependence to wave-vector dependence is explained, and is illustrated by a number of examples. The correlation of polytype properties with hexagonality is also considered.

*The research reported in this paper was sponsored in part by the Air Force Cambridge Research Laboratories, Office of Aerospace Research, under Contract AF 19(628)-68-C-0272, but the report does not necessarily reflect endorsement by the sponsor.

I. INTRODUCTION

The semiconductor properties of n-type SiC have a strong dependence on polytype. On the other hand, many other SiC properties show little or no polytype dependence. The object of this paper is to classify physical properties in a way that provides a qualitative explanation of the degree of their polytype dependence. For this purpose, properties are put into three classes, A, B, and C, according to a certain aspect of their wave-number dependence. The relationship between polytype dependence and wave-number dependence is found by considering the polytype structure in reciprocal space, as determined by the positions and structure factors of the planes of energy discontinuity. Class A properties can be further classified by polytype hexagonality (percent h) in an empirical scheme that apparently accounts for the effects of anisotropy. Both classifications can be used not only for SiC polytypes, but also for the similar family of ZnS polytypes.

Examples of the three wave-number dependent classes of properties are given in Table I. We define the classes as follows -

(A) Class A properties depend on wave vectors at the origin of the large zone ($k = 0$), or along the zone axis ($k_z \neq 0$). Only small polytype differences are expected.

(B) Class B properties depend on a symmetrically related set of wave vectors at the large zone boundary. Such properties may show large polytype differences.

(C) Class C properties depend on a weighted average over all wave vectors. These poltype differences are usually small, but occasionally the large weighting of a particular set of wave vectors leads to significant poltype differences.

TABLE I

Wave-Vector Classification
of SiC Physical Properties

A. Axial or zero wave vector

1. Direct energy gap at zone center
2. Hole masses and mobilities
3. X-ray coincidences
4. Axial phonon dispersion curves
5. Axial acoustic velocities

B. Zone-boundary wave vector

1. Indirect energy gaps
2. Electron masses and mobilities
3. Exciton luminescence
4. N-type dichroism
5. Crystal growth?

C. Weighted average over $\underset{\sim}{k}$

1. Dielectric function
2. Reflectivity
3. Birefringence
4. Thermal conductivity and expansion
5. Thermal expansion anomaly

The classification according to hexagonality or "percent h" introduces an order parameter defined by the hk polytype notation.[1] It serves to correlate the small class A differences that cannot be explained by their wave-number dependence. The essential factor appears to be a regular increasing anisotropy of many properties with increasing hexagonaltiy.

II. LARGE ZONE STRUCTURE

Polytype comparisons in reciprocal space (k space) are facilitated by the use of standard large zones.[2,3] An axial dimension of $N\pi/c$ is chosen, where N is the number of atomic layers in the stacking sequence (the number that appears in the Ramsdell symbol NH or NR). $N\pi/c$ is a constant, independent of polytype, for the unit cell dimension c is proportional to N. Thus, we compare polytypes in zones of the same volume.

This is an extension of the method that Birman[4] used to compare the band structures of the two fundamental ZnS polytypes, 3C (zincblende) and 2H (wurtzite). He chose one of the threefold zincblende axes to align with the unique wurtzite axis.* This method of comparing corresponding regions of k space in the 3C and 2H structures was again shown to be significant in recent band structure calculations for ZnS.[5,6]

When the standard large zone is used for the higher polytypes, it is cut by many planes of energy discontinuity (hereafter called E-D planes). This is illustrated for polytype 33R in Fig. 1, which shows half of a large-zone mirror plane. The zone axis is at the left. All other lines indicate the traces of E-D planes, including those that form the boundaries of the zone (heavy lines). The planes are of two

---

*Choosing one of the threefold axes is equivalent to considering cubic SiC as the basic rhombohedral polytype, i.e. as 3R instead of 3C.

kinds, horizontal and oblique, and we must consider the character and the effects of these two sets of E-D planes in order to make polytype comparisons.

The horizontal lines represent E-D planes of the form (000,3n) with integral n. However, in calculating structure factors it is common practice to use a single atomic scattering factor for all Si atoms, and another for all C atoms, and to consider all interplanar spacings equal. In this approximation all of the (000,3n) structure factors vanish except for (000,±33), which correspond to the top and bottom boundaries (heavy lines in Fig. 1). Thus, the dashed horizontal lines represent E-D planes made possible by the lower translational symmetry of polytype 33R, but for which the energy discontinuities are, in fact, very small because the true structure differs only slightly from the ideal tetrahedral structure. The corresponding X-ray reflections have not been observed. There is no comparable strength limitation on the other set of E-D planes, the set indicated by the oblique lines which form the complex network at the right of Fig. 1.

In the standard large zone of any polytype there is a similar grouping into two sets of E-D planes.* In all cases the interior planes perpendicular to the axis represent extremely small discontinuities, whereas the top and bottom boundaries correspond to the strong (000,±N) reflections, which have the same normalized structure factors for all poltypes. The second set of E-D planes corresponds to the oblique lines of Fig. 1, but the number of planes, the positions, and the structure factors of this set all vary from one polytype to another.

We conclude that the large zone of any polytype shows a central region free of strong E-D planes, top and bottom of equally strong (000,±N) planes, and a set of oblique E-D planes that is characteristic of the polytype. The part of k-space showing distinct polytype

*The number of E-D planes in both sets increases with increasing size of the unit cell. Cubic SiC has no interior E-D planes. In hexagonal, as opposed to rhombohedral polytypes, the structure factors of some of the planes perpendicular to the axis vanish identically because of the hexagonal symmetry.

characteristics is therefore the neighborhood of the large zone boundary, excluding that part formed by the (000,±N) planes. These common structural features of polytypes lead to the A, B, C classification of properties.

If the periodic crystal potential is regarded as a perturbation[7] it is clear that, for a given wave vector, polytype differences are associated with differences in nearby E-D planes. Since there are no such differences along the large zone axis, in the usual structure factor approximation, one expects only small polytype differences for class A properties. On the other hand, a conduction band minimum near the large-zone boundary occurs at a critical point which, in going from one polytype to another, is shifted in both position and energy by the changing configuration of oblique E-D planes. Consequently, there may be large differences for class B properties.

The argument given here is only qualitative, but many experimental results in both SiC and ZnS polytypes can be understood on the basis of this classification. Some properties depending on the E-D planes (or reciprocal lattice points) are X-ray reflections, electronic structure, phonon dispersion curves, and the many physical properties that depend indirectly on electrons and phonons.

III. EXPERIMENTAL RESULTS

In this section we review some experimental results that throw light on the polytype dependence of the property measured. We discuss the examples listed in Table I, following the same order.

A. Class A

The SiC zone center energy gaps (A1) have not been measured, but the ZnS band gaps are at the zone center, and they show a polytype variation of only 3% of the gap.[8] Polytype comparisons of hole masses and mobilities (A2) have not been made in either SiC or ZnS polytypes. Only small differences are expected except perhaps for cubic. The

valence band of the cubic form is unique because of its higher symmetry, hence higher degeneracy. The X-ray coincidences (A3) for (000,±N) reflections are well known,[9] and will not be discussed.

Raman scattering measurements[10] show that a single set of axial phonon dispersion curves (A4) is satisfactory, within 1%, for four polytypes (Fig. 2). The equivalence of axial acoustic velocities (A5) follows from this result. In these measurements doublets were observed that indicate small energy discontinuities at E-D planes of the form (000,3n) for which the structure factors vanish in the usual approximation (except when 3n = N). Thus, exact calculations must indeed consider the small changes in atomic scattering factors and interplanar spacings permitted by crystal symmetry. These changes result in small polytype-dependent distortions of the basic tetrahedral structure.

The measured class A differences are all small, and they are probably related to the small tetrahedral distortions. They can be correlated empirically with "percent h", and will be considered further in Sec. IV.

B. Class B

The indirect gaps of SiC polytypes (B1) vary from 2.39 to 3.33 eV.[11,12] The conduction band minima are at the X positions in cubic SiC,* in the region of the large zone where E-D planes have a strong dependence on polytype. It is not surprising, then, that the corresponding minima change, with changing polytype, in position, in number, and in energy. All electronic properties, such as masses and mobilities (B2) therefore depend strongly on polytype. Considerable differences were reported in the electron mobilities of 6H, 15R, and 4H polytypes.[13] Mass and mobility anisotropies have not yet been measured, but are expected to show a strong polytype dependence also.

---

*This position in the standard large zone is shown in Fig. 4 of Ref. 2.

The energies in the SiC luminescence spectra depend on polytype because of the energy gaps, and so do phonons emitted in the indirect transitions, because of the changing positions of the conduction band minima. Therefore, highly complex and characteristic spectra[14] are observed for exciton recombination radiation (B3).

N-type samples of SiC polytypes show a striking dichroism (B4) because of direct transitions from the conduction band minima to higher minima.[15] Since both initial and final states have $\underset{\sim}{k}$ vectors on polytype. The most familiar of these are the ordinary ray colors ($E \perp c$) because the typical platelet is thin in the direction of the optic axis. One observes green in 6H, yellow in 15R, the depth of color depending on the density of electrons in the conduction band or on donor atoms.

The most striking polytype differences in SiC are due to the positions of the conduction band minima, as indicated above. No such differences are observed in the direct-gap ZnS polytypes. Although polytype series are known in some other materials, none compares with SiC in variability of physical properties.

The listing of crystal growth here (B5) is speculative. It is meant to suggest that, in determining the structure of a crystal nucleus, a small class B contribution to the free energy, with its strong polytype dependence, may be as significant as a much larger class A or C contribution with weak polytype dependence.

The growth of high polytypes is usually attributed to the growth spiral mechanism,[1] but there are four or five basic forms that probably result from thermodynamic considerations. They have different, but overlapping ranges of growth temperatures.[16] Little is known about the more significant nucleation temperatures. It seems likely that there is a very delicate balance of free energies, with several contributing factors. Our discussion will be confined to one possible class B contribution.

The sharpest growth temperature boundary seems to be that between 2H below 1430°C and cubic above.[12] This is a change from the polytype with the largest energy gap to that with the smallest. It is therefore marked by a large increase in carrier populations. The (negative) free energy contribution of holes and electrons is quite insignificant at low temperatures, and even at 1430°C it is very much smaller than that of the lattice vibrations, but the latter is class C and probably has a very small polytype dependence. Thus, the relatively small energy gap of cubic SiC may favor its appearance in this temperature range.

C. Class C

The dielectric function (C1) involves all $\underset{\sim}{k}$ vectors, but is strongly weighted for photon energies near direct transition thresholds. Thus, a class C property may have some class A or B character near a threshold if the transition occurs at a $\underset{\sim}{k}$ vector on the axis (A) or the zone boundary (B). The low-frequency dielectric constant has been measured only for 6H SiC,[17] but is likely to be independent of polytype to a good approximation.

The dielectric function controls the reflectivity (C2) which should have the same general appearance in all polytypes, but distinctive detail wherever the zone-boundary direct transition structure can be resolved. Similarities in SiC polytype reflectivities have been stressed by Wheeler,[18] but some distinctive polytype differences have been found.[19] For ZnS polytypes also, a general similarity but some distinct differences in reflectivity were found by Baars.[20]

The dielectric function also determines the birefringence (C3), which has been measured for many ZnS polytypes.[8] However, the measurements were made at 5460 Å, where the zone-center transitions may be dominant, giving the birefringence more of a class A character. Thus, the correlation with hexagonality is expected.

Thermal conductivity and thermal expansion (C4) are expected to have little polytype dependence except for a slight anisotropy which

may vary with hexagonality. However, a distinct thermal expansion anomaly (C5) was found in 6H SiC.[21] From 400 to 1000°K there is preferential expansion along the c axis. This is probably due to the high density of phonon states associated with the flat, low-frequency, planar acoustic branch in the axial direction. The phonon dispersion curves[10] indicate a density of states peak in the frequency spectrum at 265 cm^{-1} (380°K), which apparently lies below all other such peaks. Thus, at 400°K there is a preferred population of modes propagating along the crystal axis, leading to a preferred expansion direction which persists until the optical phonon branches are excited.

IV. CORRELATION WITH "PERCENT h"

The wave-vector classification makes no reference to the observed tetrahedral distortions, and explains no class A polytype differences. These minor differences are correlated in a very satisfactory manner by the empirical "percent h" scheme. It works, not only for SiC and ZnS polytypes, but also for certain metallic alloys which form structures analogous to polytypes. The alloy correlations have been discussed by Hodges.[22]

If neighbors beyond the second are ignored, Si or C sites in any polytype have neighborhoods of two kinds, h or k, which are like those in the cubic (k) or 2H (h) structures. The planes in the polytype stacking sequence may then also be labeled h or k, leading to the hk polytype notation,[1] from which one can obtain immediately the percentage of h planes. This is the order parameter against which class A properties are plotted.

Figure 3 shows that, for several SiC polytypes, the anisotropy in the transverse optical phonon energies, and the c/a axial ratios are both proportional to "percent h". In ZnS polytypes a similar relation exists for the direct energy gaps and for the birefringence. As noted above, the birefringence measured near the direct gap at k = 0 may have the character of a class A property.

Most of the small class A differences appear to be determined by the polytype anisotropy, which seems to vary between the limits for cubic (3C) and wurtzite (2HO in a regular manner that is adequately described by the "percent h". Whether class C properties may also be correlated with "percent h" has not yet been established. At one time the correlation appeared to hold for a class B property, the SiC indirect gaps,[11] but it failed to predict the 2H gap.[12] On reflection, there does not appear to be any reason for the correlation to hold for class B properties.

REFERENCES

1. A.R. Verma and P. Krishna, Polymorphism and Polytypism in Crystals (John Wiley and Sons, Inc., New York, 1966).

2. D. R. Hamilton, Lyle Patrick and W. J. Choyke, Phys. Rev. 138, A1472 (1965).

3. W. J. Choyke, D. R. Hamilton and Lyle Patrick, Phys. Rev. 139, A1262 (1965).

4. J. L. Birman, Phys. Rev. 115, 1493 (1959).

5. M.L. Cohen and T.K. Bergstresser, Phys. Rev. 141, 789 (1966).

6. T.K. Bergstresser and M.L. Cohen, Phys. Rev. 164, 1069 (1967).

7. H. Jones, The Theory of Brillouin Zones and Electronic States in Crystals (North-Holland Publishing Co., Amsterdam, 1960), p. 180.

8. O. Brafman and I.T. Steinberger, Phys. Rev. 143, 501 (1966).

9. F.G. Smith, AM. Mineralogist 40, 658 (1955). See also Ref. 1.

10. D.W. Feldman, James H. Parker, Jr., W.J. Choyke and Lyle Patrick, Phys. Rev. 173, (1968).

11. W.J. Choyke, D.R. Hamilton and Lyle Patrick, Phys. Rev. 133, A1163 (1964).

12. Lyle Patrick, D.R. Hamilton and W.J. Choyke, Phys. Rev. 143, 526 (1966).

13. D.L. Barrett and R.B. Campbell, J. Appl. Phys. 38, 53 (1967).

14. W.J. Choyke, this volume.

15. E. Biedermann, Solid State Comm. 3, 343 (1965).

16. W.F. Knippenberg, Philips Res. Repts. 18, 161 (1963).

17. W.J. Choyke and Lyle Patrick, J. Opt. Soc. Am. 58, 377 (1968).

18. B.E. Wheeler, Solid State Comm. 4, 173 (1966).

19. W.J. Choyke, Lyle Patrick and M. Cardona, Bull. Am. Phys. Soc. 11, 764 (1966).

20. J.W. Baars, in II-VI Semiconducting Compounds, edited by D.G. Thomas (W.A. Benjamin, Inc., New York, 1967), p. 631.

21. A. Taylor and R.M. Jones, in Silicon Carbide, edited by J.R. O'Connor and J. Smiltens (Pergamon Press, Inc., New York, 1960), p. 147.

22. C.H. Hodges, Acta Met. 15, 1787 (1967).

FIGURE CAPTIONS

Fig. 1 Half a mirror plane of a large zone for 33R SiC. The heavy line is the zone boundary. Lighter lines represent energy discontinuities, of which there are two kinds. Those corresponding to the broken horizontal lines are extremely weak, but others, indicated by oblique lines, are strong.

Fig. 2 Axial phonon dispersion curves in a standard large zone. One set of curves fits the Raman scattering data of four SiC polytypes.

Fig. 3 Two measures of polytype anisotropy in SiC plotted against "percent h". (a) The closed circles represent the anisotropy of the transverse optical phonon modes (TO_1-TO_2), from Raman measurements. (b) Open circles are reduced c/a axial ratios for polytypes 6H and 2H, from X-ray measurements.

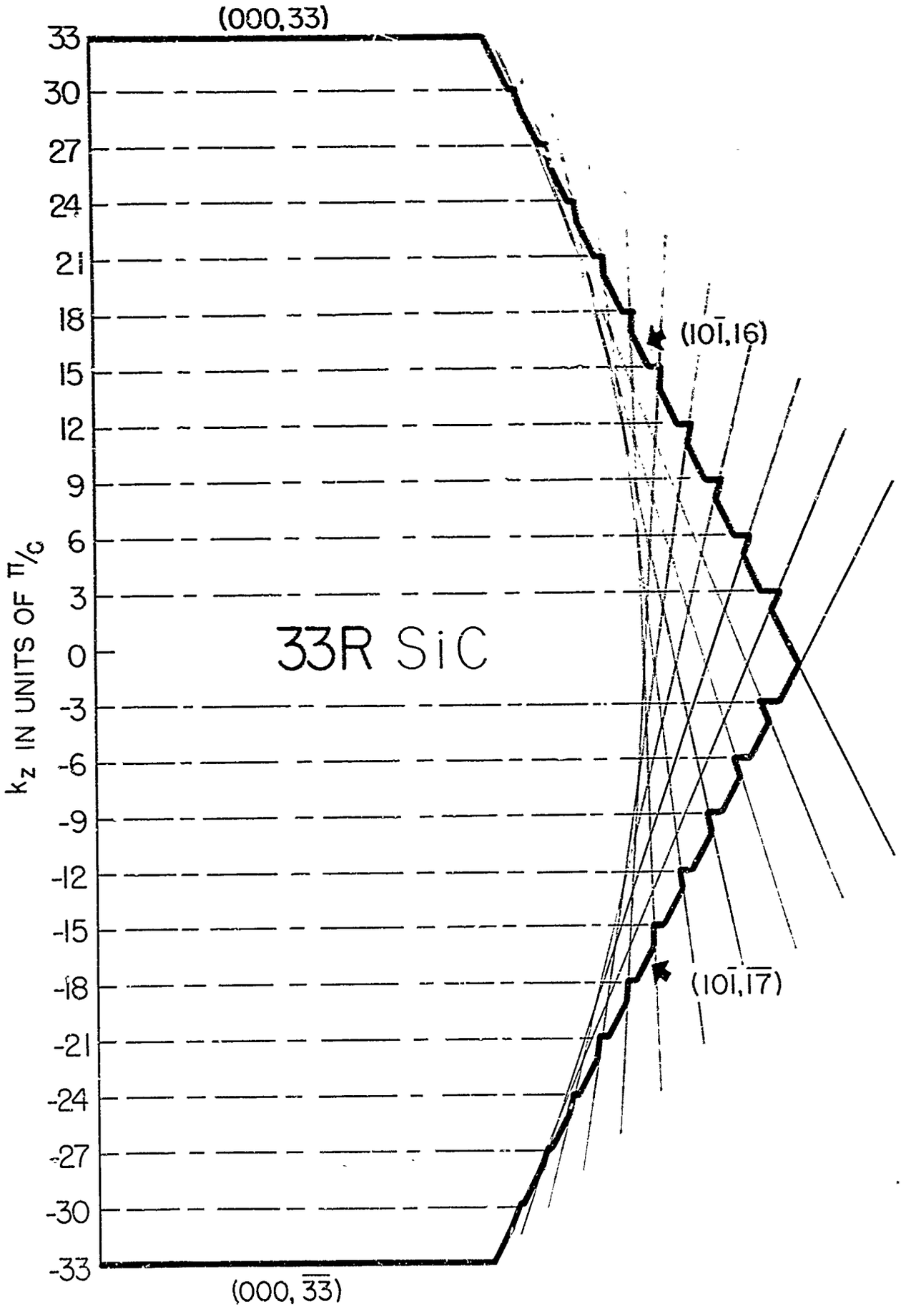
(000,33)
33
30
27
24
21
18
15
12
9
6
3
0
-3
-6
-9
-12
-15
-18
-21
-24
-27
-30
-33
(000, $\overline{33}$)
k_z IN UNITS OF π/c
33R SiC
(10$\bar{1}$,16)
(10$\bar{1}$,$\overline{17}$)

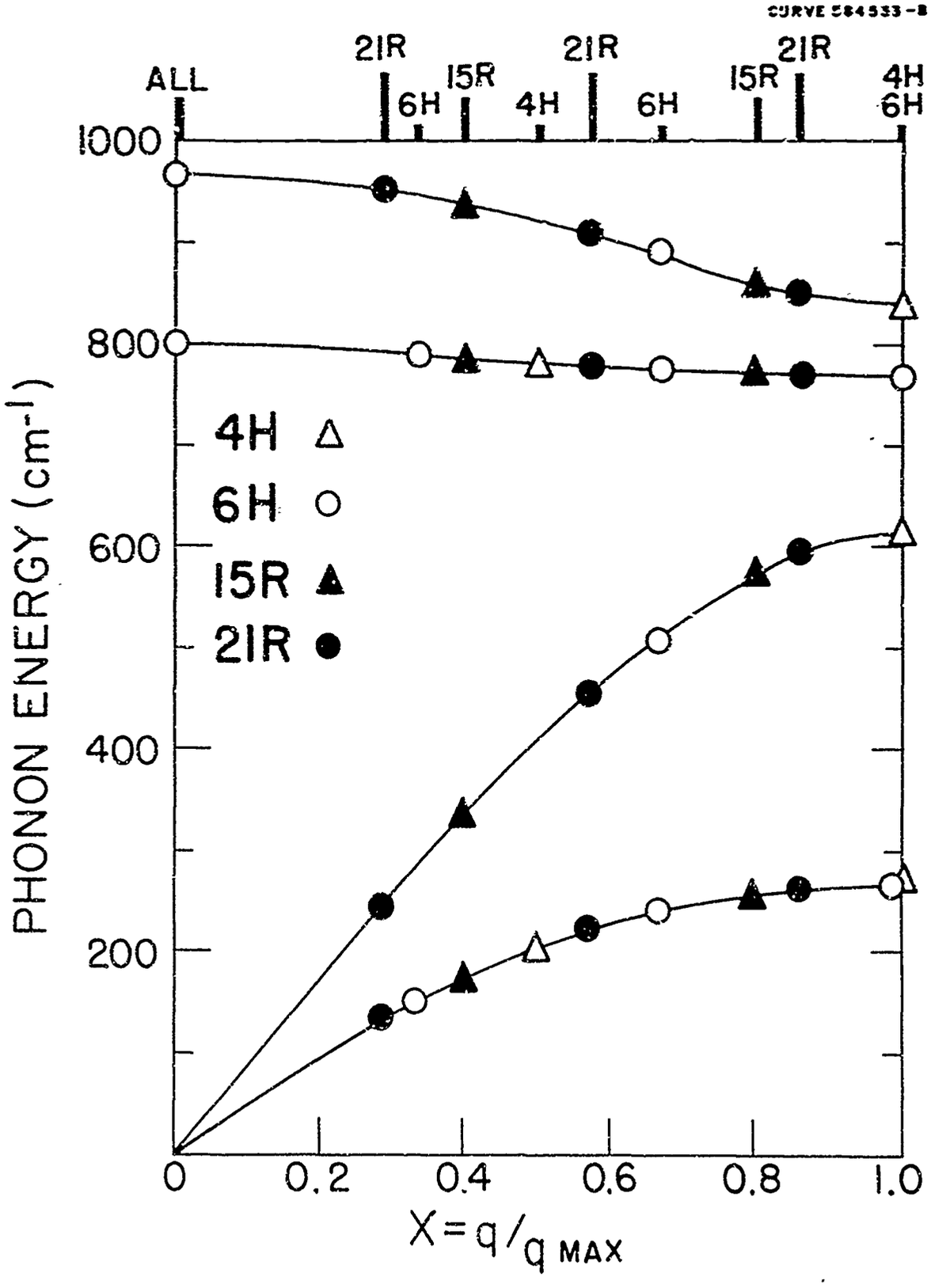
CURVE 584533-B
ALL
21R
6H
15R
4H
21R
6H
15R
21R
4H
6H
1000
800
600
400
200
PHONON ENERGY (cm⁻¹)
4H △
6H ○
15R ▲
21R ●
0
0.2
0.4
0.6
0.8
1.0
X = q/q MAX

Fig. 2

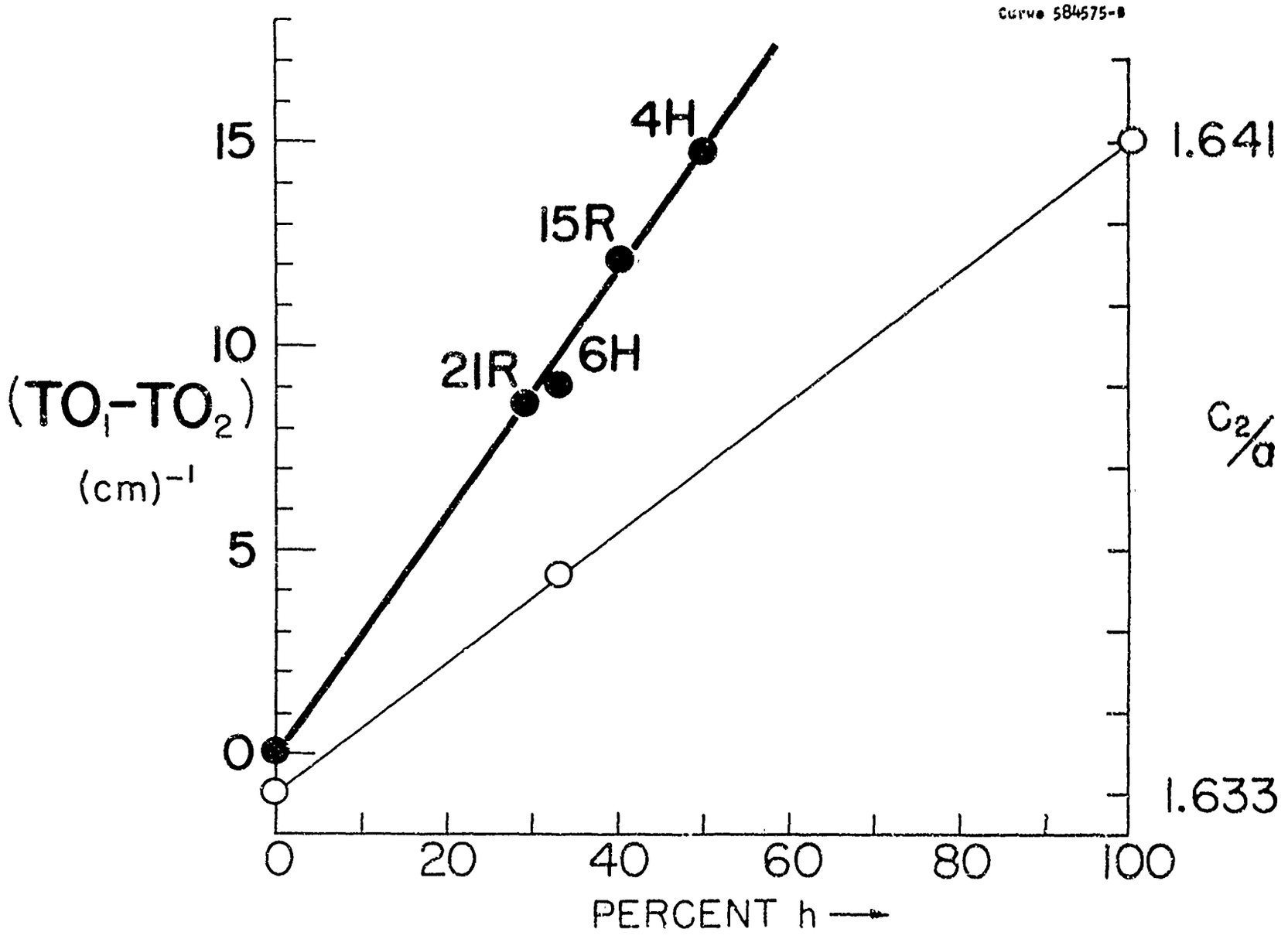
Curve 584575-B
15
10
5
0
(TO_1-TO_2)
$(cm)^{-1}$
4H
15R
21R
6H
1.641
1.633
c_2/a
0
20
40
60
80
100
PERCENT h ⟶

Fig. 3

APPENDIX D -- Optical Properties of Polytypes of SiC: Interband Absorption, and Luminescence of Nitrogen-Exciton Complexes

October 15, 1968

OPTICAL PROPERTIES OF POLYTYPES OF SiC: INTERBAND ABSORPTION, AND LUMINESCENCE OF NITROGEN-EXCITON COMPLEXES*

W. J. Choyke

Westinghouse Research Laboratories
Pittsburgh, Pennsylvania 15235

Abstract

A summary is given of the optical absorption in seven polytypes of SiC. Nitrogen-exciton four-particle and three-particle spectra for a number of polytypes are discussed. Combining energies from four-particle and three-particle no-phonon data to yield values for donor ionization energies is reviewed.

---

*The research reported in this paper was sponsored in part by the Air Force Cambridge Research Laboratories, Office of Aerospace Research, under Contract AF 19(628)-68-C-0272, but the report does not necessarily reflect endorsement by the sponsor.

I. INTRODUCTION

Since the last SiC Conference almost ten years ago, considerable effort, all over the world, has been spent on studying the optical properties of this fascinating family of polytypes. To review critically so much work in so little space is fruitless both to the reader and to the writer, the latter having to bear the abuse from authors who feel they have not been fairly cited. Consequently, we choose to summarize some of the results obtained in our laboratories during this ten-year interval, keeping in mind the current interest in junction devices.

II. ABSORPTION SPECTRUM

The absorption edges of seven polytypes of SiC are shown in Fig. 1. The shape of the edges is characteristic of indirect transitions which create excitons. As is customary for indirect transitions,[1] we have plotted the square root of the absorption coefficient against photon energy. Only the phonon emission part is significant at 4.2°K and only the "principal" phonons give rise to resolvable structure. Absorption curves for $E \parallel C$ have also been obtained but the structure is not as well resolved as for $E \perp C$ and in general the absorption is weaker.[2]

The structure marked by letters and arrows in Fig. 1 is due to emission of some of the "principal" phonons, which have wave vector

$\vec{k}$ at the large zone boundary, and have very similar energies in all the polytypes shown except 2H.[3] The phonon energies are obtained much more accurately from luminescence measurements (Sec. III), and it is the combined information from absorption and luminescence which gives us the values of the exciton energy gaps (E_{GX}) indicated by arrows on the abscissa in Fig. 1.

All the absorption edges except 2H can be approximately superimposed after an energy shift and multiplication of α by an appropriate factor. This is a consequence of the nearly identical "principal" phonon energies in these polytypes. In the case of 2H the phonon energies are different and no superposition is possible. Nevertheless, a rough comparison of absorption strengths is still possible, and we find a ten-to-one variation among the polytypes. This is an example of a Class B property.[4]

In Fig. 2 we give values for the exciton energy gap E_{GX} at 4.2°K for eight polytypes. The temperature dependence of E_{GX} over a considerable range of temperature has been measured only for 4H, 6H, 15R, and 21R. The solid lines indicate range of actual measurement of E_{GX} whereas the dashed lines indicate a rough estimate of the temperature dependence. The temperature variation of E_{GX} is obtained from absorption measurements by observing, at low temperatures, the break in the curve which indicates the beginning of the phonon emission part; and at high temperatures the break which indicates the beginning of the phonon absorption part. All structure in the absorption edge becomes less distinct with increasing temperature; hence, the high temperature portion

of Fig. 2 is somewhat uncertain. The assumed similarity of the temperature dependence of E_{GX} for all the polytypes is based on the similarity of their phonon spectra.

Recent reflectivity studies on 6H SiC in the ultraviolet have shown some weak structure at 4.6 eV but were inconclusive as to whether this structure is of an intrinsic nature and whether it is associated with a direct transition at 4.6 eV[5,6] Optical absorption measurements on very thin crystals provide an alternative experimental technique for examining structure in this region. One is able to grow thin samples of a few microns thickness and prepare samples as thin as 1.8μ.[7]

Figure 3 shows absorption measurements on 6H SiC to nearly 4.9 eV. The typical crystal habit of hexagonal SiC restricts measurements to one polarization direction ($E \perp C$), but this is the direction for which the reflectance measurements were made. The results show three successive indirect edges, indicated by E_{G_1}, E_{G_2}, and E_{G_3} in Fig. 3 and a fourth absorption edge E_{G_4} at 4.6 eV. E_{G_4} also appears to be indirect but one cannot be certain since it becomes increasingly difficult to distinguish between direct and indirect edges as one goes to higher energies. An indirect edge at 4.6 eV is incapable of explaining the reported structure in the reflectivity. One must conclude at this stage that the character of the 4.6 eV edge has not yet been established.

III. EXCITON RECOMBINATION RADIATION

The mechanism of exciton recombination for an indirect semiconductor is illustrated schematically in Fig. 4. For a bound

exciton, the hole at $\vec{k} = 0$ and the electron at $\vec{k} = \vec{k}_{CB}$ may recombine without phonon emission in some fraction of the transitions. This gives rise to very sharp lines termed, "no-phonon lines". In SiC polytypes with multiple donor sites, the relative strength of a no-phonon line shows a direct correlation with the binding energy, E_{4x}, by which an exciton is bound to a neutral donor. In other transitions crystal momentum is preserved by emission of a phonon which either scatters the electron to an intermediate conduction-band state at $\vec{k}_o$, or scatters the hole to an intermediate valence-band state at $\vec{k}_{CB}$. Many recombination channels are available, because either the electron or the hole scattering may be to one of several bands of intermediate states. Those bands are favored which most nearly conserve energy in the intermediate state.[1]

In Table I we summarize, for 8 polytypes of SiC, the theoretically possible number of no-phonon and one-phonon lines that one might expect to see in the luminescence spectrum of a four particle nitrogen-exciton complex. The large unit cells of polytypes 4H, 6H, 8H, 15R, 21R, and 33R have several sites, not required to be equivalent by crystal symmetry. If the effective mass approximation for shallow donors[9] in these polytypes is inexact, we expect to obtain one no-phonon line and a family of one-phonon lines for each inequivalent site. The simplest spectrum is obtained for cubic SiC since it has the fewest atoms in the unit cell of any polytype. In Fig. 5 we show its four particle nitrogen-exciton complex spectrum. There are 5 strong narrow lines which are labeled according to the phonon emitted in the transition, with "0"

TABLE I

Total number of no-phonon and one-phonon lines theoretically observable in a four particle nitrogen-exciton complex spectrum of 3C, 8H, 21R, 15R, 33R, 6H, 4H and 2H SiC.

Polytype (SiC)	Atoms of C and Si in the Unit Cell	Number of Phonon Branches (Neglecting Degeneracy)	Inequivalent Sites in the Unit Cell	Bound Exciton Lines		
				No-Phonon		One-Phonon
3C	2	6	I	I	+	6
8H	16	48	IV	IV	+	192
21R	14	42	VII	VII	+	294
15R	10	30	V	V	+	150
33R	22	66	XI	XI	+	726
6H	12	36	III	III	+	108
4H	8	24	II	II	+	48
2H	4	12	I	I	+	12

indicating that in which no phonon is emitted. The exciton energy gap E_{GX}, determined from absorption measurements, is indicated by the heavy arrow in Fig. 5. The displacement of the "0" peak from E_{GX} is 10 meV, and is a measure of the energy by which the exciton is bound to the nitrogen. The small value of this binding energy is one indication that the complex is formed by an exciton and a neutral nitrogen (to form a four particle complex). The binding of an exciton to ionized nitrogen

to form a three particle complex would be comparable with the ionization energy of the nitrogen (perhaps 100 meV).[10] A three-particle spectrum has not been observed in cubic SiC whereas it is quite strong in 6H,[10] 33R,[11] and 15R SiC.[2]

The phonon energies derived from Fig. 5 are listed in Table II, together with the principal phonons in 21R, 15R, 33R, 6H, 4H, and 2H SiC.

TABLE II

Comparison of principal phonon energies in seven polytypes. Energies in meV. T = transverse, A = acoustic, L = longitudinal, O = optic.

Phonon Branch	Cubic	21R	15R	33R	6H	4H	2H	
TA_1	46.3	46.5	46.3	46.3	46.3	46.7	52.5	A
TA_2		53	51.9	52.3	53.5	< 51.4, 53.4	61.5	A
LA	79.5	77.5	78.2	77.5	77.5	< 76.9, 78.8		
TO_1	94.4	94.5	94.6	94.7	94.7	95.0	91.2	
TO_2			95.7	95.7	95.6		100.3	O
LO	102.8	104	103.7	103.7	104.2	< 104.0, 104.3	103.4	O

For cubic SiC the notation for transverse acoustic (TA), longitudinal acoustic (LA), transverse optical (TO), and longitudinal optical (LO) is accurate, since the cubic conduction band minima are on the symmetry axes.[12] For the hexagonal and rhombohedral polytypes

the notation is somewhat inaccurate, but convenient. When using the large zone, the number of phonon energies assigned to each branch is TA $[2\ (\frac{3n}{6})]$, LA $[\ \frac{3n}{6}\ ]$, TO $[2\ (\frac{3n}{6})]$, and LO $[\ \frac{3n}{6}\ ]$ where n is the number of atoms in the unit cell, as given in Table I. Neglecting polytype 2H for the moment let us compare the principal phonon for cubic, 21R, 15R, 33R, 6H, and 4H. Here we compare 6 polytypes with 3 different symmetries, whose phonons have $\vec{k}$ vectors which are determined by the positions of the conduction-band minima. For the transverse phonons the agreement is essentially within experimental error. In the case of the longitudinal phonons there appears to be a slight trend in the sequence cubic, 21R, 15R, 33R, 6H, 4H: namely, LA decreases while LO increases.

The calculation of Herman, Kortum and Kuglin[12] for cubic SiC places the conduction-band minima at X, i.e. at the zone boundary in < 100 > directions. Hence in cubic SiC the two TA momentum conserving phonons should be degenerate, and likewise, the two TO phonons. This is consistent with the data in Fig. 5 where we find 4 rather than 6 phonons. In addition, our previous comparison of the principal phonons indicates that the conduction-band minima of the other polytypes are likely to be at the large zone boundaries. Thus we have three conduction-band minima for cubic SiC and probably 12 minima for 4H and 6H and 6 minima for 33R, 15R, and 21R.

In 2H SiC[3] the experimental data can be used together with symmetry arguments to place 2 conduction-band minima at the K positions of the Brillouin zone.

We shall now consider two Lampert complexes[13] in greater detail, namely: (a) an exciton bound to a neutral donor (four-particle complex, or (4)), and (b) an exciton bound to a donor ion (three-particle complex, or (3)). In Fig. 6 we give both Lampert's pictorial notation and ours, and in terms of this notation we define six dissociation or binding energies.[10] The energies required to remove excitons from four- or three-particle complexes, E_{4x} and E_{3x}, can be expressed in terms of the independent energies defined by the first and fourth equation in Fig. 6. Hence we can obtain the relations: $E_{4x} = E_{3x} + E_3 - E_x$ and $E_{3x} = E_3 + E_i - E_x$. By combining these relations we get an expression for the donor ionization energy: $E_i = E_{3x} - E_{4x} + E_4$. Our measurements give accurate values for E_{3x} and E_{4x}. An estimate of E_4 can only be obtained rather indirectly, as outlined in Sec. VI of Ref. 10 for a 6H donor. Figure 6 also shows levels which represent possible relative energies of various combinations of the particles which form a four-particle complex.

We are now in a position to compare, in Fig. 7, the observed (4) and (3) particle nitrogen exciton no-phonon spectra of 2H, 4H, 6H, 33R, 15R, 21R and 3C SiC.

In 2H a very weak (4) no-phonon line was observed at 3.320 eV, giving a value of E_{4x} of 10 meV. Notably absent for 2H SiC is the (3) particle spectrum.

For 4H SiC at 6°K we have two (4) no-phonon lines with E_{4x} values of 7 meV and 20 meV. At about 20°K the 7 meV line disappears because of thermal dissociation of the complex. An examination of about

fifty 4H samples showed, in every case, a (3) particle spectrum stable up to 77°K which, however, is almost certainly <u>not</u> due to nitrogen. In other crystals of 4H SiC many narrow-spaced sharp lines were also observed and appear to be similar to donor-acceptor pair lines seen in GaP.[14,15]

In 6H SiC at 6°K we observe three (4) no-phonon lines with binding energies of 16, 31, and 33 meV. At 15°K the 16 meV line is about half its 6°K value, and all three lines have disappeared by 77°K. Contrary to the previous situation in 2H and 4H, we have a strong (3) nitrogen spectrum in 6H. As we have already noted on Fig. 6, the binding energy E_{3x} is large compared to E_{4x} and the exciton binding energy E_x. Hence for 6H SiC we have three (3) no-phonon lines with E_{3x} of 162, 203, and 237 meV.

For 33R SiC we would expect 11 (4) no-phonon lines since nitrogen is almost certainly distributed over the 11 sites, but we observe only 10. Even at very low temperatures the eleventh line was not observed, and it is unlikely to be concealed in an unresolved doublet. It is thought to be missing because of too small a value of E_{4x}. The values of E_{4x} range from 9.2 to 33.2 meV. Some lines are so close together that they are not shown resolved in Fig. 7. As in 6H SiC there is a strong (3) nitrogen spectrum visible up to 77°K. We see 9 (perhaps 10) lines with E_{3x} ranging from 142 to 220 meV.

For 15R we should expect 5 (4) no-phonon lines but we show only four in Fig. 7. The missing line is believed to be associated with the "same" site as that responsible for the missing (4) no-phonon line

in 33R SiC.[11] The E_{4x} values are 7, 9, 19, and 20 meV. As in 6H and 33R we also have a strong (3) nitrogen spectrum but it is no longer visible at 77°K. This accounts for the fact that under U.V. illumination at 77°K 6H and 15R nitrogen-doped samples will have a distinctly different color. The measured values of E_{3x} are 125, 148, 158, and 199 meV.

The 21R luminescence spectrum at 6°K of (4) nitrogen exciton complexes yields 6 instead of an expected 7 no-phonon lines.[16] As in the case of 33R and 15R it is possible that the binding energy to the seventh site is very small. However, a spectrum taken at 1.6°K did not reveal a seventh line. The values of E_{4x} in 21R range from 10 to 40 meV. No trace of a (3) spectrum was observed.

Finally, we have the single no-phonon line for cubic SiC which has already been discussed in connection with Fig. 5. Again we see no (3) particle spectrum. Four of the seven spectra shown in Fig. 7 do <u>not</u> have a (3) spectrum associated with the (4) spectrum. Possible reasons for the absence of three-particle complexes have been advanced by several authors.[17,18,19,20]

Lastly, we should like to make some general remarks about the rather complicated nitrogen-exciton luminescence spectra which are actually observed. A schematic of such a spectrum for 6H SiC is shown in Fig. 8. In addition to the no-phonon lines already discussed, we may have phonon lines associated with the free exciton, and a phonon spectrum associated with each type of complex. That obtained from the (4) particle spectrum is characteristic of a loosely bound center, and that obtained from the (3) particle spectrum is characteristic of a tightly

bound center. At higher temperatures, lines due to thermally excited states of the complexes are observed. The excited states of the (4) particle complexes, in general, appear to be due to the presence of a second valence band (spin-orbit splitting) while those of the (3) particle complexes are attributed to valley-orbit splitting. However, additional complications can arise such that the final state is one in which the donor electron is <u>not</u> in the lowest valley-orbit state.

In the case where one is able to observe both a (4) particle and (3) particle nitrogen-spectrum, such as in 6H, 33R, and 15R, one is able to make estimates of the donor ionization energies E_i. As an example we take 6H SiC as shown on the right side of Fig. 8. Recalling the relationship $E_i = E_{3x} - E_{4x} + E_4$ and pairing the no-phonon lines A with P, B with R, and C with S, we obtain three values for $E_{i(\text{minimum})}$. Using a value of 25 meV for E_4 [10] we obtain probable values for the donor ionization energies of 170, 200, and 230 meV.

IV. CONCLUSIONS

Much has been learned about the absorption spectra of SiC and the luminescence spectra of nitrogen-exciton complexes. However, our understanding of other impurity spectra in SiC is far less advanced. Higher transitions are still poorly understood and await good band calculations. Donor-acceptor pair spectra abound but their unravelling awaits a far more sophisticated understanding of the energy levels of the donors and acceptors which are involved. Hopefully, in another ten years we shall have another SiC Conference and then the band structure

and "zoology" of many impurities in SiC will be fully understood. This will not only be intellectually satisfying but will, without doubt, make possible far greater utilization of SiC for device applications.

REFERENCES

1. T.P. McLean, in Progress in Semiconductors (Heywood and Company, Ltd., London, 1960), Vol. 5, p. 55.
2. Lyle Patrick, D.R. Hamilton and W.J. Choyke, Phys, Rev. 132, 2023 (1963).
3. Lyle Patrick, D.R. Hamilton and W.J. Choyke, Phys. Rev. 143, 529 (1966).
4. Lyle Patrick, this volume.
5. B.E. Wheeler, Solid State Comm. 4, 173 (1966).
6. W.J. Choyke, Lyle Patrick and M. Cardona, Bull. Am. Phys. Soc. 11, 764 (1966).
7. W.J. Choyke and Lyle Patrick, Phys. Rev. 172, 769 (1968).
8. W.J. Choyke and Lyle Patrick, Phys. Rev. 127, 1868 (1962).
9. W. Kohn, in Solid State Physics, edited by F. Seitz and D. Turnbull (Academic Press Inc., New York, 1957), Vol. 5, p. 257.
10. D.R. Hamilton, W.J. Choyke and Lyle Patrick, Phys. Rev. 131, 127 (1963).
11. W.J. Choyke, D.R. Hamilton and Lyle Patrick, Phys. Rev. 139, A1262 (1965).
12. F. Herman, R.L. Kortum and C.D. Kuglin, Int. J. Quantum Chem. 1S, 533 (1967).
13. M.A. Lampert, Phys. Rev. Letters 1, 450 (1958).
14. J.J. Hopfield, D.G. Thomas and M. Gershenzon, Phys. Rev. Letters 10, 162 (1963).

15. Donor-acceptor pair-like spectra have been observed in many SiC polytypes.

16. D.R. Hamilton, Lyle Patrick and W.J. Choyke, Phys. Rev. 138, A1472 (1965).

17. J.J. Hopfield, in Proceedings of the International Conference of the Physics of Semiconductors, Paris, 1964 (Dunod, Paris, 1964), p. 725.

18. W.J. Choyke, Lyle Patrick and D.R. Hamilton, Ref. 17, p. 751.

19. R.R. Sharma and S. Rodriguez, Phys. Rev. 153, 823 (1967).

20. M. Suffczynski and W. Gorzkowski, "II-IV Semiconducting Compounds," edited by D.G. Thomas, Benjamin, New York (1967), p. 384.

FIGURE CAPTIONS

Fig. 1 Absorption edge of polytypes 3C, 21R, 15R, 33R, 6H, 4H, and 2H SiC at 4.2°K, for light polarized $E \perp C$. The structure is characteristic of indirect exciton-creating transitions. Only the phonon emission part is observed at this temperature, and the resolved structure is due to the emission of a small number of "principal" phonons.

Fig. 2 Temperature dependence of the 2H, 4H, 6H, 33R, 15R, 21R, 8H, and cubic exciton energy gap, E_{GX}. Solid lines indicate range of actual measurements. Dashed lines indicate a rough estimate of the temperature dependence. The usual gap E_G, is given by $E_G = E_{GX} + E_X$, where E_X is the still unknown exciton binding energy.

Fig. 3 Plot of $\alpha^{1/2}$ versus $h\nu$ at 300°K with light polarized $E \perp C$ and data from many samples. Measured values fall on straight-line segments (solid), or in transitional regions (dotted). The four arrows indicate the estimated values of E_G.

Fig. 4 Schematic of indirect exciton recombination for a semiconductor with valence band (V.B.) maximum at $k = 0$ and conduction band (C.B.) minimum at $k = k_{CB}$. The no-phonon transition occurs only for bound excitons. Other recombination modes require both an optical (vertical) transition and an electron or hole scattering, going through a number of intermediate states in which energy need not be conserved.

Fig. 5 The luminescence spectrum of four-particle nitrogen-exciton complexes in cubic SiC at 6°K. The phonon-free line is labeled "0" and its energy is used as the zero for the upper "phonon energy" scale, from which one may read directly the energies of TA, LA, TO, and LO phonons. The 10 meV between "E_{GX}" and "0" is a measure of the binding energy of the exciton to the nitrogen atom.

Fig. 6 Energy-level diagram, notation, and definitions. The levels represent possible relative energies of various combinations of the particles which form a four-particle complex. The complex itself is the lowest level, being the most strongly bound combination. The top level represents the completely separated particles. The distance between levels gives the binding energies defined by the equations on the left of the figure.

Fig. 7 Observed no-phonon lines in (4) and (3) particle nitrogen exciton spectrum of 2H 4H, 33R, 15R, 21R, and 3C SiC.

Fig. 8 A diagram showing the energy ranges of the two distinct 6H nitrogen-exciton (4) and (3) particle spectra, and indicating the positions of the three no-phonon lines in each spectrum. Pairing lines A with P, B with R, and C with S we obtain three values for $E_{i(\text{minimum})}$. $E_{i(\text{probable})}$ may be obtained from the relation $E_{i(\text{probable})} = E_{3x} - E_{4x} + (\approx 25 \text{ meV})$.

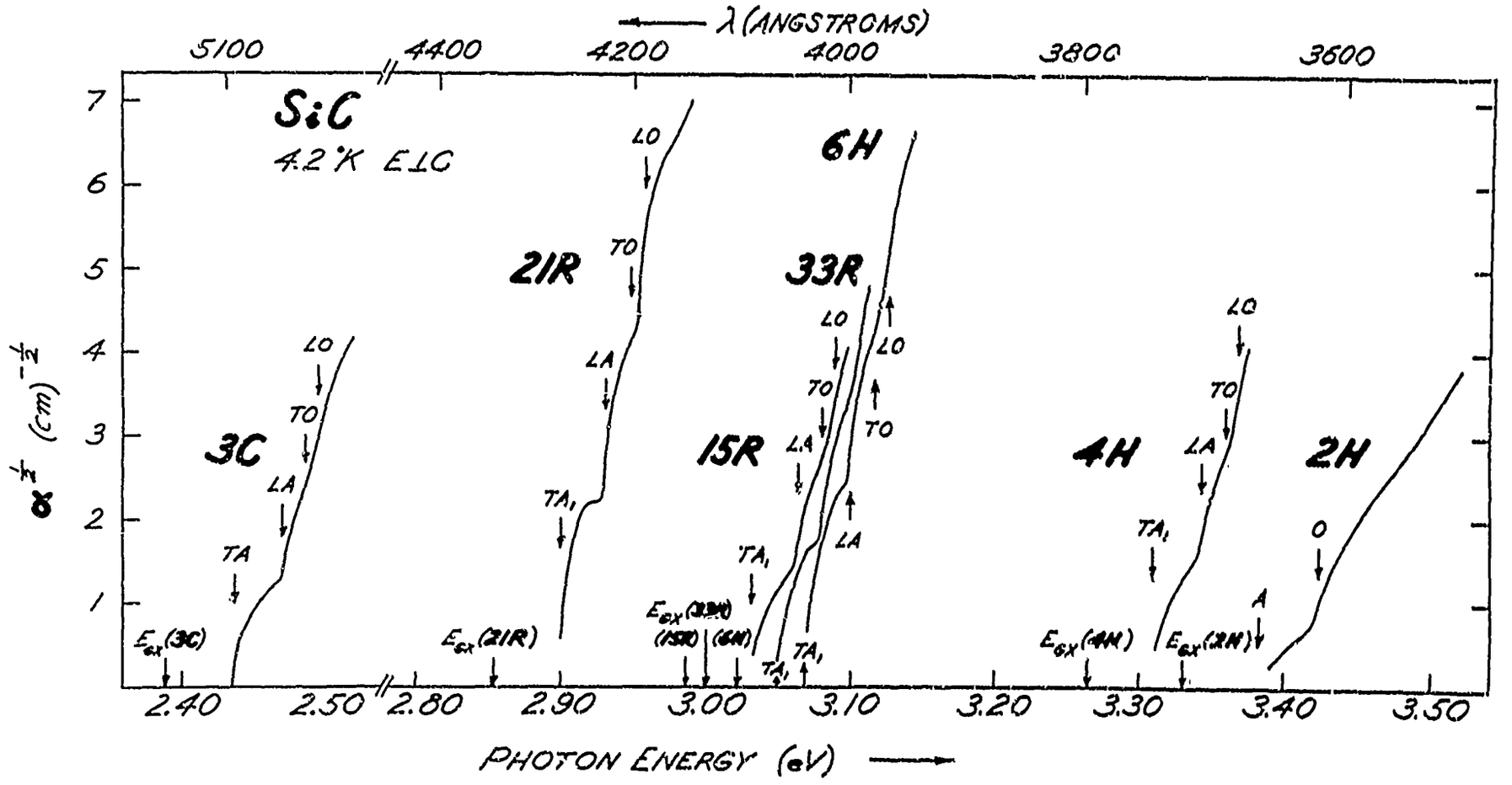
λ (ANGSTROMS)
5100
4400
4200
4000
3800
3600
SiC
4.2°K E⊥C
3C
2IR
6H
33R
15R
4H
2H
LO
TO
LA
TA
TA₁
O
A
E_{ex}(3C)
E_{ex}(2IR)
E_{ex}(4H)
E_{ex}(2H)
$\alpha^{\frac{1}{2}}$ (cm)$^{-\frac{1}{2}}$
1
2
3
4
5
6
7
2.40
2.50
2.80
2.90
3.00
3.10
3.20
3.30
3.40
3.50
PHOTON ENERGY (eV)

FIG. 1

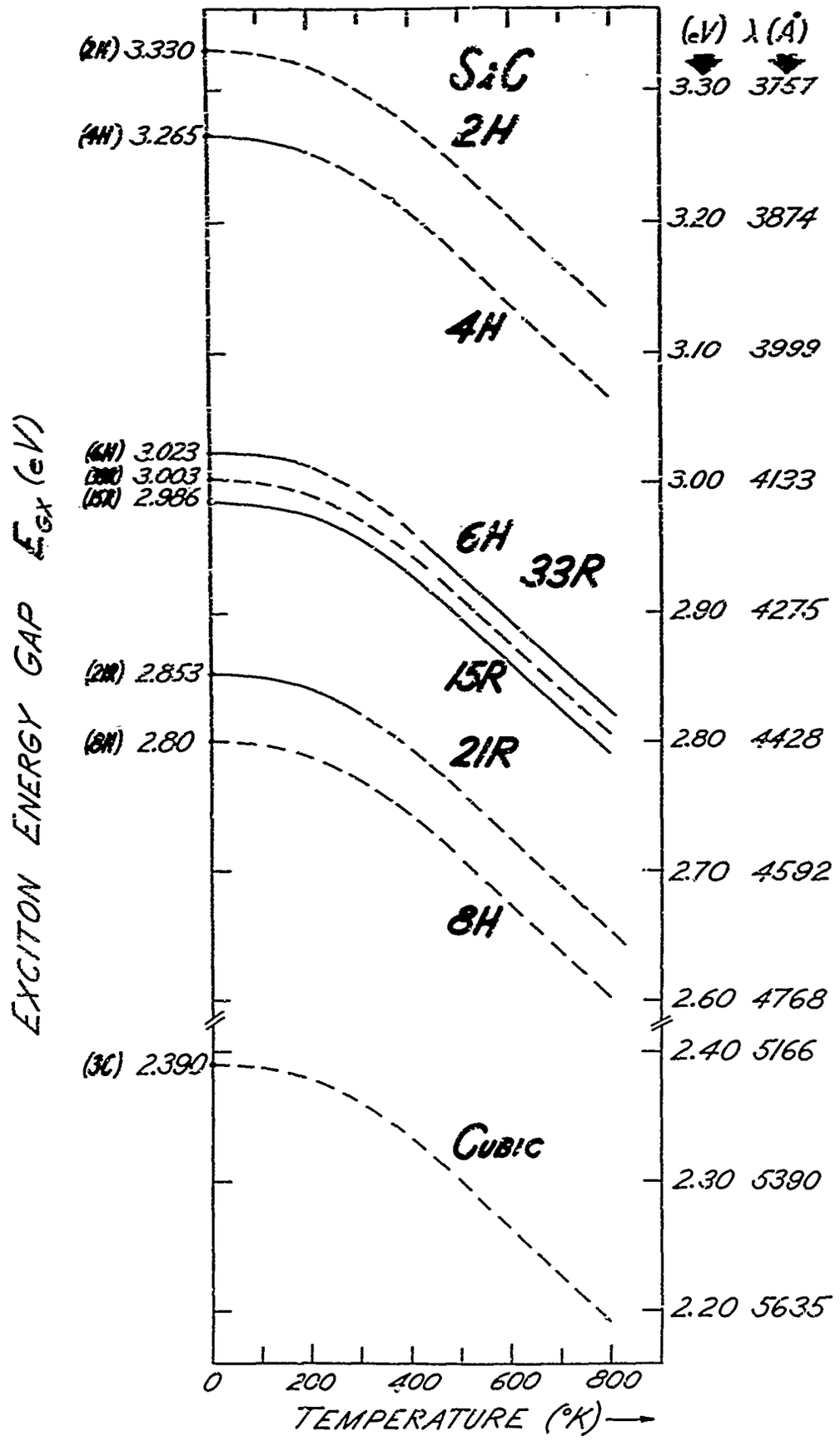
SiC
2H
4H
6H
33R
15R
21R
8H
Cubic
(2H) 3.330
(4H) 3.265
(6H) 3.023
(33R) 3.003
(15R) 2.986
(21R) 2.853
(8H) 2.80
(3C) 2.390
(eV) λ (Å)
3.30 3757
3.20 3874
3.10 3999
3.00 4133
2.90 4275
2.80 4428
2.70 4592
2.60 4768
2.40 5166
2.30 5390
2.20 5635
EXCITON ENERGY GAP E_{GX} (eV)
0 200 400 600 800
TEMPERATURE (°K)

FIG. 2

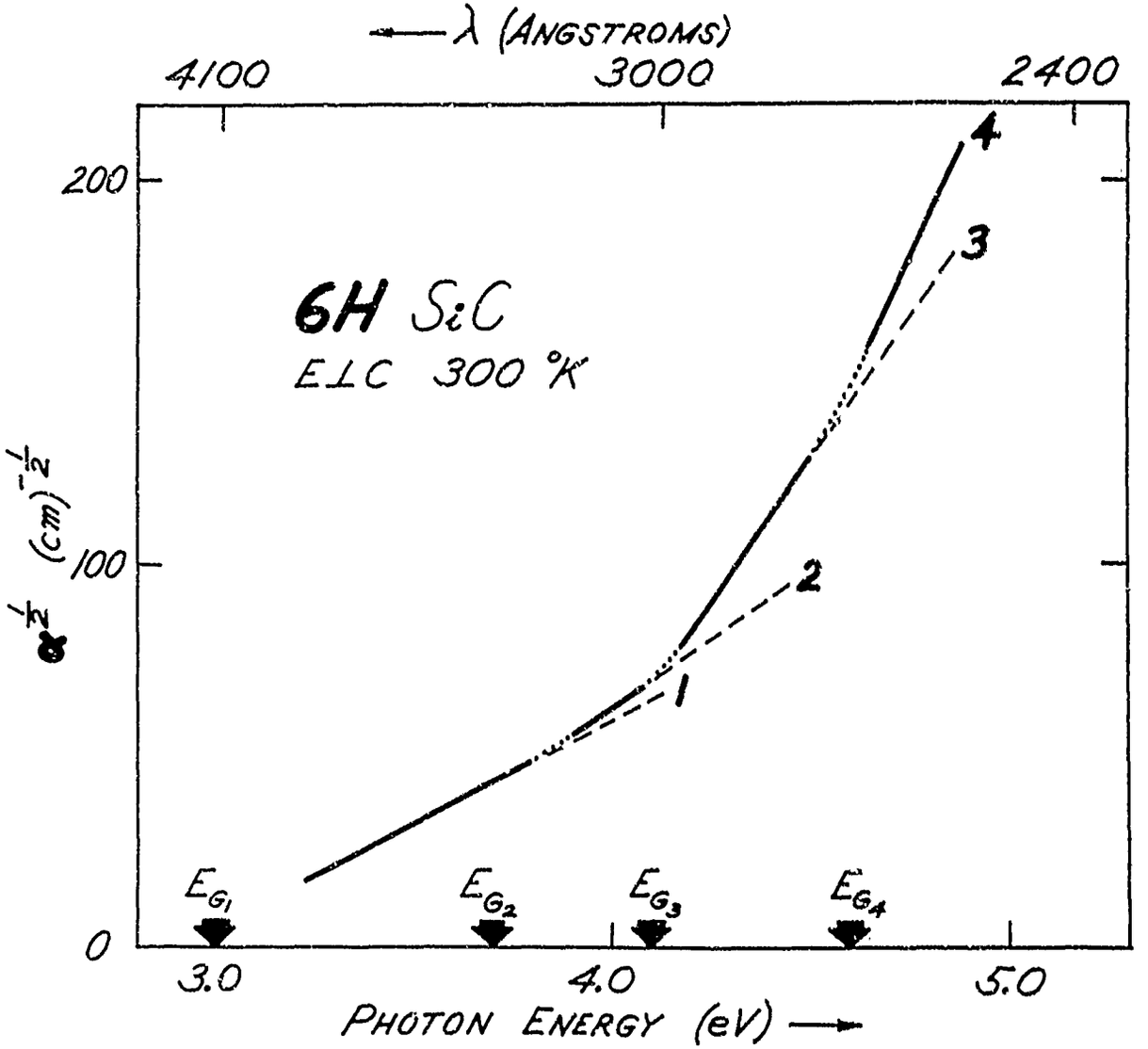
λ (ANGSTROMS)
4100
3000
2400
200
100
0
6H SiC
E⊥C 300 °K
$\alpha^{\frac{1}{2}}$ (cm)$^{-\frac{1}{2}}$
1
2
3
4
E_{G_1}
E_{G_2}
E_{G_3}
E_{G_4}
3.0
4.0
5.0
PHOTON ENERGY (eV)

FIG. 3

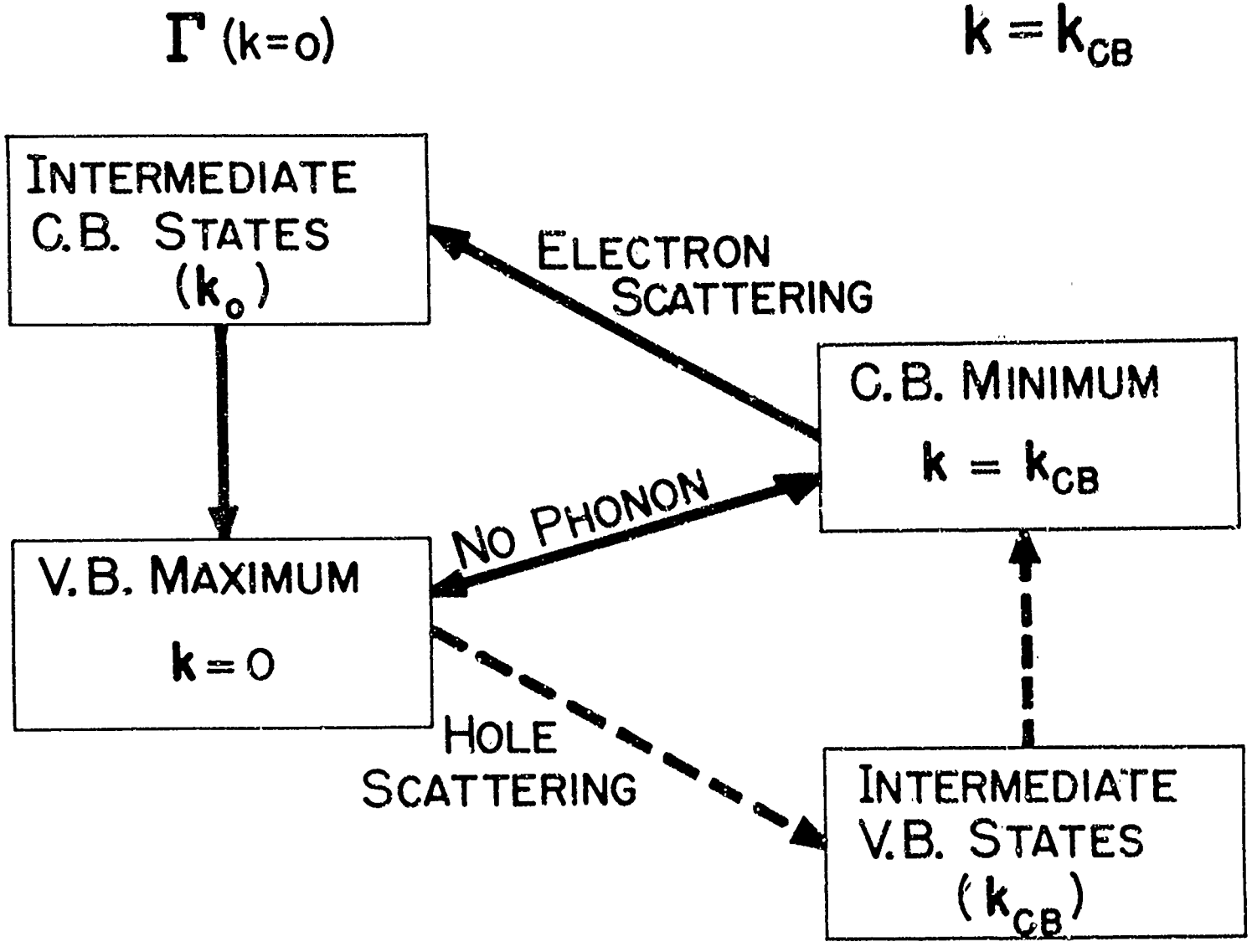
Γ (k=0)
k = k_CB
INTERMEDIATE C.B. STATES (k_o)
ELECTRON SCATTERING
C.B. MINIMUM k = k_CB
NO PHONON
V.B. MAXIMUM k=0
HOLE SCATTERING
INTERMEDIATE V.B. STATES (k_CB)

FIG. 4

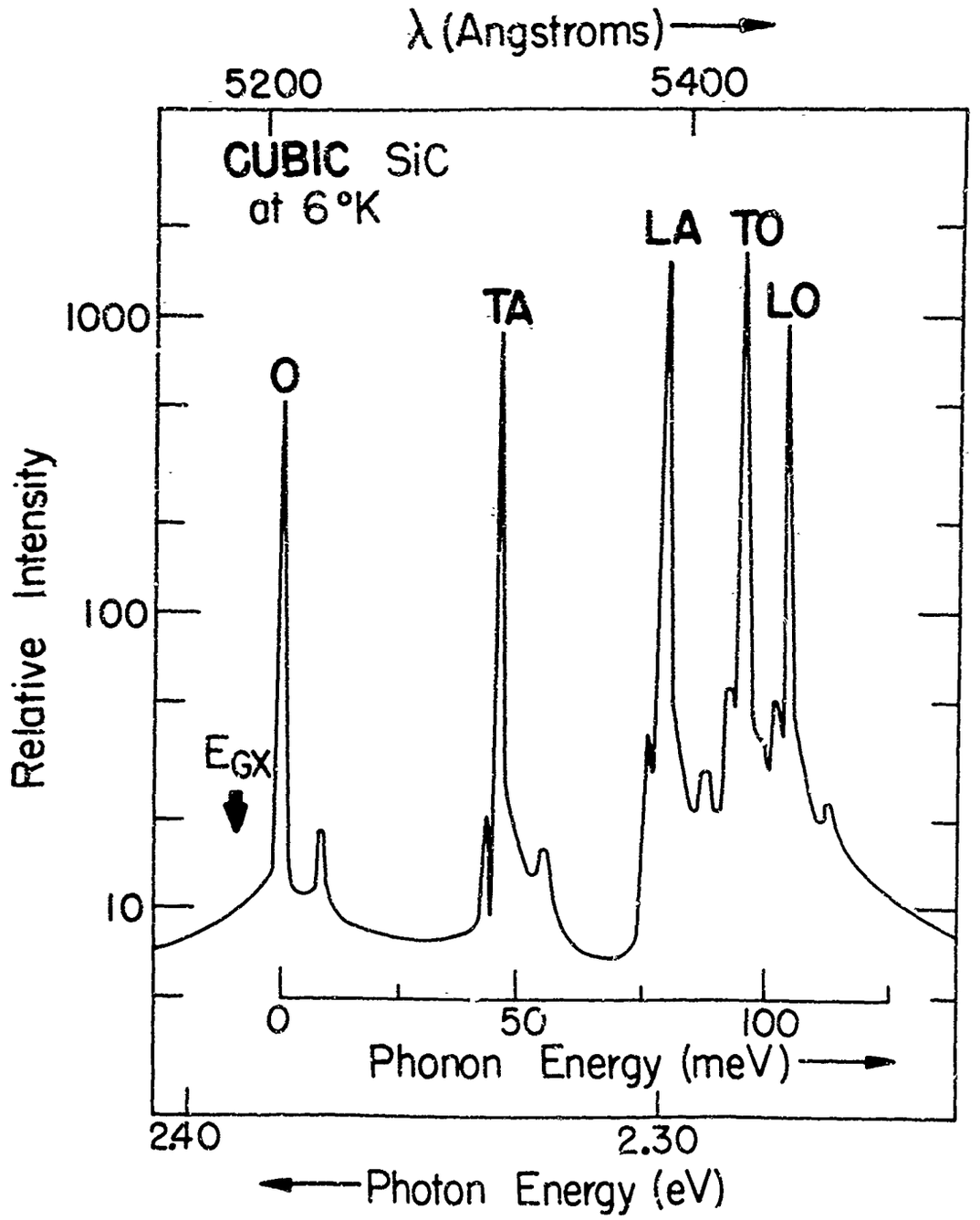
λ (Angstroms)
5200
5400
CUBIC SiC
at 6°K
LA
TO
LO
TA
O
1000
100
10
Relative Intensity
EGX
0
50
100
Phonon Energy (meV)
2.40
2.30
Photon Energy (eV)

FIG. 5

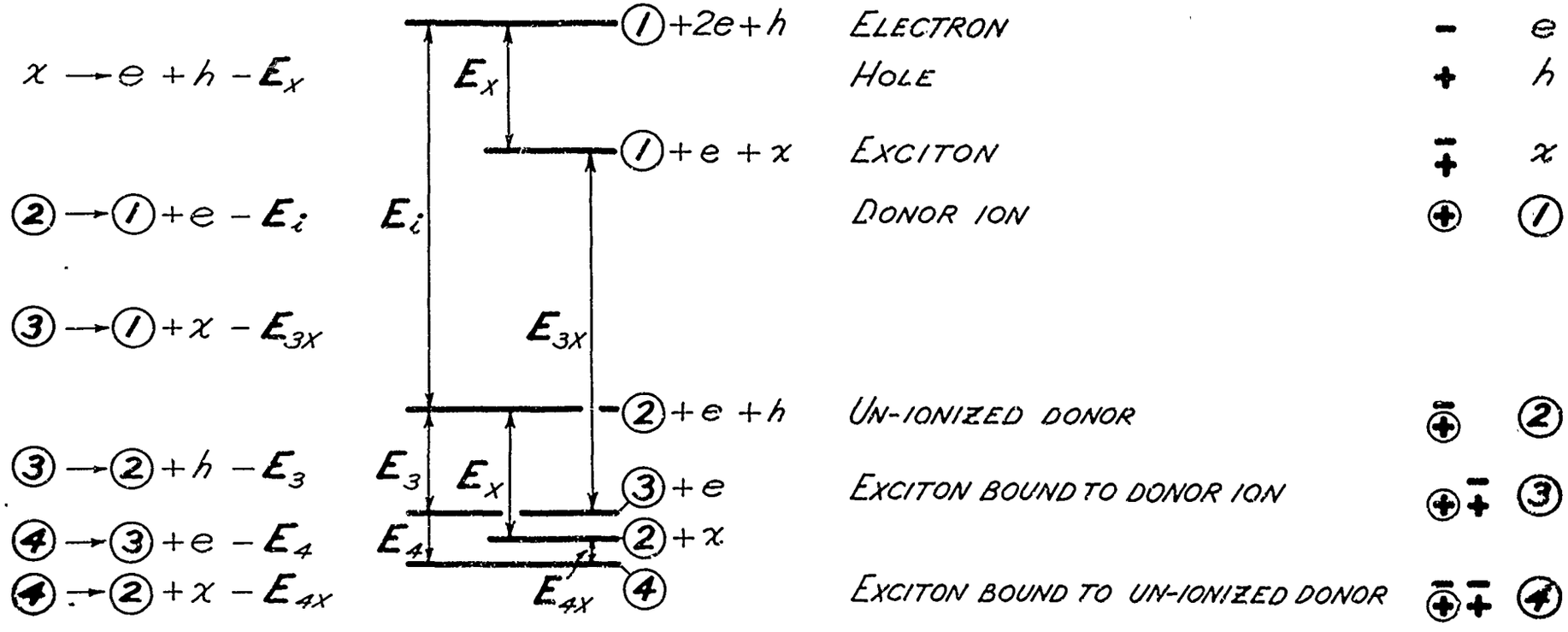
$x \rightarrow e + h - E_x$
E_x
① + 2e + h
ELECTRON
e
HOLE
h
① + e + x
EXCITON
x
② → ① + e − E_i
E_i
DONOR ION
①
③ → ① + x − E_{3X}
E_{3X}
② + e + h
UN-IONIZED DONOR
②
③ → ② + h − E_3
E_3
E_x
③ + e
EXCITON BOUND TO DONOR ION
③
④ → ③ + e − E_4
E_4
② + x
④ → ② + x − E_{4X}
E_{4X}
④
EXCITON BOUND TO UN-IONIZED DONOR
④

FIG. 6

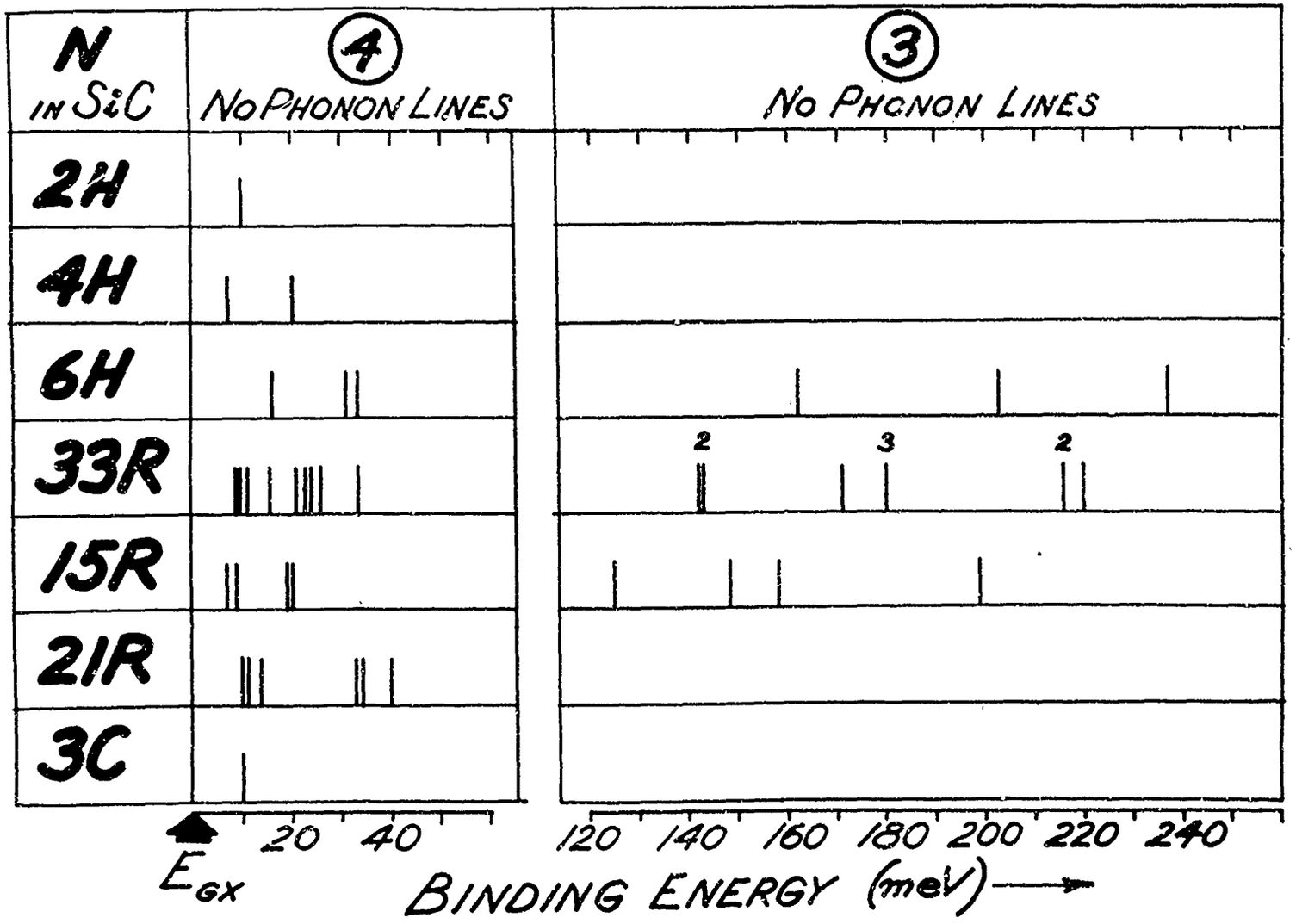
N
IN SiC
4
NO PHONON LINES
3
NO PHONON LINES
2H
4H
6H
33R
15R
21R
3C
2
3
2
20
40
120
140
160
180
200
220
240
E_{GX}
BINDING ENERGY (meV)

FIG. 7

N IN 6H SiC

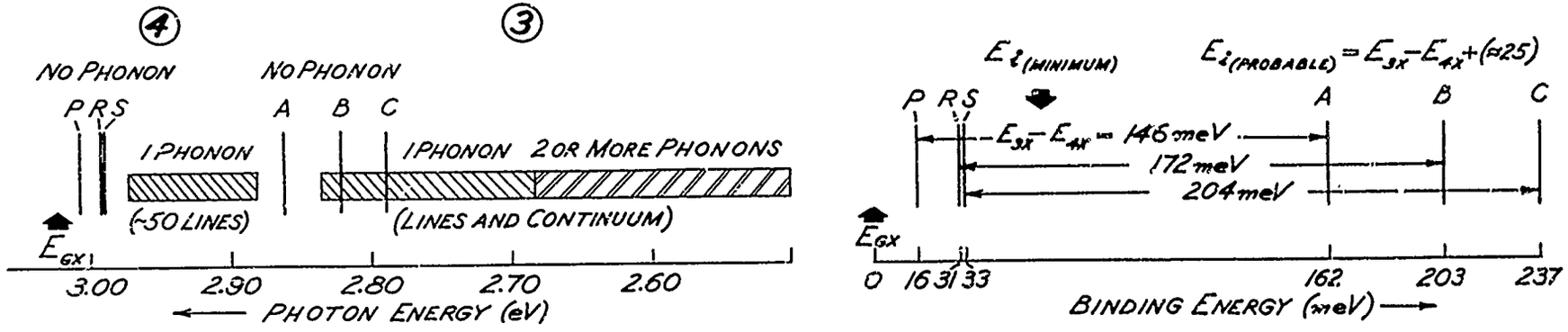

FIG. 8

UNCLASSIFIED

Security Classification

DOCUMENT CONTROL DATA - R&D

(Security classification of title body of abstract and indexing annotation must be entered when the overall report is classified)

1. ORIGINATING ACTIVITY (Corporate author) Westinghouse Research Laboratories Pittsburgh, Pennsylvania 15235	2a. REPORT SECURITY CLASSIFICATION Unclassified 2b GROUP

3 REPORT TITLE

OPTICAL PROPERTIES OF 4H, 6H, 15R, 21R, CUBIC SiC

4. DESCRIPTIVE NOTES (Type of report and inclusive dates)

Final Report. 1 April 1968 - 31 March 1969 Approved 28 July 1969

5. AUTHOR(S) (Last name, first name, initial)

Choyke, Wolfgang J. and Patrick, Lyle

6. REPORT DATE	7a. TOTAL NO. OF PAGES	7b. NO. OF REFS
30 April 1969	89	75

8a. CONTRACT OR GRANT NO. F19628-68-C-0272 b. PROJECT NO. Task, Work Unit Nos. 5620-08-01 c. DoD Element 6144501F d DoD Subelement 681301	9a. ORIGINATOR'S REPORT NUMBER(S) 9b. OTHER REPORT NO(S) (Any other numbers that may be assigned this report) AFCRL-69-0181

10. AVAILABILITY/LIMITATION NOTICES

1 - Distribution of this document is unlimited. It may be released to the Clearinghouse, Department of Commerce, for sale to the general public.

11. SUPPLEMENTARY NOTES	12. SPONSORING MILITARY ACTIVITY
TECH, OTHER	Air Force Cambridge Research Laboratories Office of Aerospace Research Bedford, Massachusetts 01730

13. ABSTRACT

Optical absorption and reflectivity studies were carried out on a variety of cubic SiC samples. Two additional indirect transitions at 3.55 eV and 4.2 eV have been found. In N-type cubic SiC the inter-conduction band transition X_{1c} to X_{3c} has been accurately located. Results have been compared with recent band calculations of Herman, Van Dyke and Kortum.

Two additional papers were prepared dealing with a general discussion of the dependence of the physical properties on polytype structure and the optical properties of polytypes of SiC.

DD FORM 1 JAN 64 1473

UNCLASSIFIED

Security Classification

RM 35054

14. KEY WORDS	LINK A		LINK B		LINK C	
	ROLE	WT	ROLE	WT	ROLE	WT
Polytypes Optical Instrumentation Absorption Reflectivity Energy Cap Transitions Physical Complex Silicon Carbide Properties						

INSTRUCTIONS

1. ORIGINATING ACTIVITY: Enter the name and address of the contractor, subcontractor, grantee, Department of Defense activity or other organization *(corporate author)* issuing the report.

2a. REPORT SECURITY CLASSIFICATION: Enter the overall security classification of the report. Indicate whether "Restricted Data" is included. Marking is to be in accordance with appropriate security regulations.

2b. GROUP: Automatic downgrading is specified in DoD Directive 5200.10 and Armed Forces Industrial Manual. Enter the group number. Also, when applicable, show that optional markings have been used for Group 3 and Group 4 as authorized.

3. REPORT TITLE: Enter the complete report title in all capital letters. Titles in all cases should be unclassified. If a meaningful title cannot be selected without classification, show title classification in all capitals in parenthesis immediately following the title.

4. DESCRIPTIVE NOTES: If appropriate, enter the type of report, e.g., interim, progress, summary, annual, or final. Give the inclusive dates when a specific reporting period is covered.

5. AUTHOR(S): Enter the name(s) of author(s) as shown on or in the report. Enter last name, first name, middle initial. If military, show rank and branch of service. The name of the principal author is an absolute minimum requirement.

6. REPORT DATE: Enter the date of the report as day, month, year; or month, year. If more than one date appears on the report, use date of publication.

7a. TOTAL NUMBER OF PAGES: The total page count should follow normal pagination procedures, i.e., enter the number of pages containing information.

7b. NUMBER OF REFERENCES: Enter the total number of references cited in the report.

8a. CONTRACT OR GRANT NUMBER: If appropriate, enter the applicable number of the contract or grant under which the report was written.

8b, 8c, & 8d. PROJECT NUMBER: Enter the appropriate military department identification, such as project number, subproject number, system numbers, task number, etc.

9a. ORIGINATOR'S REPORT NUMBER(S): Enter the official report number by which the document will be identified and controlled by the originating activity. This number must be unique to this report.

9b. OTHER REPORT NUMBER(S): If the report has been assigned any other report numbers *(either by the originator or by the sponsor)*, also enter this number(s).

10. AVAILABILITY/LIMITATION NOTICES: Enter any limitations on further dissemination of the report, other than those imposed by security classification, using standard statements such as:

(1) "Qualified requesters may obtain copies of this report from DDC."

(2) "Foreign announcement and dissemination of this report by DDC is not authorized."

(3) "U. S. Government agencies may obtain copies of this report directly from DDC. Other qualified DDC users shall request through _____."

(4) "U. S. military agencies may obtain copies of this report directly from DDC. Other qualified users shall request through _____."

(5) "All distribution of this report is controlled. Qualified DDC users shall request through _____."

If the report has been furnished to the Office of Technical Services, Department of Commerce, for sale to the public, indicate this fact and enter the price, if known.

11. SUPPLEMENTARY NOTES: Use for additional explanatory notes.

12. SPONSORING MILITARY ACTIVITY: Enter the name of the departmental project office or laboratory sponsoring *(paying for)* the research and development. Include address.

13 ABSTRACT: Enter an abstract giving a brief and factual summary of the document indicative of the report, even though it may also appear elsewhere in the body of the technical report. If additional space is required, a continuation sheet shall be attached.

It is highly desirable that the abstract of classified reports be unclassified. Each paragraph of the abstract shall end with an indication of the military security classification of the information in the paragraph, represented as *(TS), (S), (C), or (U)*

There is no limitation on the length of the abstract. However, the suggested length is from 150 to 225 words.

14 KEY WORDS: Key words are technically meaningful terms or short phrases that characterize a report and may be used as index entries for cataloging the report. Key words must be selected so that no security classification is required. Identifiers, such as equipment model designation, trade name, military project code name, geographic location, may be used as key words but will be followed by an indication of technical context. The assignment of links, rules, and weights is optional.